TALLINN UNIVERSITY OF TECHNOLOGY
SCHOOL OF ENGINEERING

Department of Materials and Environmental Technology

ADVANCED ARCHITECTED INTERPENETRATING PHASE COMPOSITE MATERIALS BASED ON IRON LATTICE STRUCTURES OBTAINED VIA SELECTIVE LASER MELTING

Master Thesis

Supervisor: Yaroslav Holovenko

Student: Jeffrey Raymond Johnson
156320KAYM

E-mail: raymond.jeffrey10@gmail.com

Study programme: Materials and Processes of Sustainable Energetics

Tallinn 2017

Author's Declaration

Hereby I declare, that I have written this thesis independently. No academic degree has been applied for based on this material. All works, major viewpoints and data of the other authors used in this thesis have been referenced.

31-05-2017

Jeffrey Raymond Johnson

.....

/signature /

Thesis is in accordance with terms and requirements

"....." 2017

Supervisor Yaroslav Holovenko

….....

/signature/

Accepted for defence

06-06-2017

Chairman of thesis defence commission: .....

/name and signature/

TALLINNA TEHNIKAÜLIKOOL
INSENERITEADUSKOND

Materjali ja keskkonnatehnoloogia instituut

LASERSULATATUD RAUA VÕREL PÕHINEVAD TÄIUSTATUD ÜLESEHITUSEGA SISSETUNGIVAD FAASILISED KOMPOSIIDMATERJALID

Magistritöö

Juhendaja: Yaroslav Holovenko

õpilane Jeffrey Raymond Johnson
156320KAYM

E-post: raymond.jeffrey10@gmail.com

õppekava: Materjalid ja protsessid
jätkusuutlikus energeetikas

Acknowledgments

I would like to express my deepest gratitude to all the people who have contributed to complete my Master Thesis. I would like to thank Mr.Yaroslav Holovenko who has given me such a beautiful opportunity to work in Mechanical Engineering Department and allotted me such a wonderful project. Their help in over viewing and designing the project is commendable.

I am grateful for the help received from Lauri Kollo and Marek Jõeleht without their help this project would not have been possible because as he taught all the necessary steps to become an efficient master student.

Thank Jesus and to my parents Nancy and Johnson. Thankful to Ajith Kumar, Heli Rihkrand, Nataly Kaur, Sri Hari, Avinash Vikatakavi, Bhavana Rangappa, Vanitha Sunil, Ruben Paul, Seshadri, Lidia Kolessova, Eliis Sootee, Sukanya Anand, Godwin and Gregory for providing me with unfailing support and continuous encouragement. I must also express my very profound gratitude to Fob solutions öu with Raigo Õunapuu, Urmas Käbi, Priit Oja and Jana Karilaid for giving me a big support to complete my thesis.

Thankful to University of Tartu and Tallinn University of Technology for giving me the opportunity of realizing my Master Thesis.

CONTENTS

Abbreviation and Acronyms

1D – 1 Dimensional

3D – 3-Dimensional

3DP – 3D printing

Al – Aluminium

CAD – Computer aided design

DC – Direct current

DMLS – Direct metal laser sintering

EDS – Energy dispersive spectroscopy

FDM – Fused deposition modelling

IPC – Interpenetrating phase composite

LOM – Laminated object manufacturing

OM – Optical microscope

SEM – Scanning electron microscope

SLM – Selective laser melting

SLSS – Elective laser sintering

SPS – Spark plasma sintering

TF – Final sintering temperature

TPMS – Triply periodic minimal surface

XRD – X-ray diffraction

1. Introduction

Since the start of the industrial revolution manufacturing process have shown rapid and escalating development. The objective of sustainable technology is to reduce simultaneously both costs and environmental impacts. It is possible to produce very complex designs by additive manufacturing. In order to obtain a good sustainable product, you need to choose the correct technologies and then to optimize the production stages. Additive manufacturing has several economic and environmental benefits over other technologies such as:

- more efficient and reduced raw wastage of materials in printing difficult parts compared to subtractive manufacturing technologies,
- very complex structures with very small features (in microns) using CAD software,
- customized and optimized designs for significantly reducing the weight of the part which is crucial in aerospace industries and lot of supply chain productions.

Architected Interpenetrating Phase Composite materials (IPC) are possible to obtain with the help of additive manufacturing (AM) technology, this in turn could be useful for different applications for sustainable energetics.

A lot of research is carried out in additive manufacturing but architected Interpenetrating Phase Composite Materials for energetics are yet to be investigated. In the current thesis production of IPC materials using AM technology is investigated. In addition, mechanical and behavioural properties of IPC are evaluated. Finally, real applications are considered and proposed for IPC materials.

2. Literature review

2.1. Architected Interpenetrating Phase Composite Materials

Interpenetrating Phase Composite is a new type of composite materials comprised of a ductile matrix reinforced with a single, continuous, periodic mathematically designed topology. In regard to the multiphase composites materials, there are already examples in nature further distinguished between discrete or continuous manner. Discrete composites are reinforced with dispersed particles or fibres with various size, shape and orientation [1]. In **Fig.2.1** It shown 4 types of IPC's materials are illustrated which have been investigated by Oraib Al-Ketan at al.

Triply Periodic minimal surface (TPMS) are mathematically created, self-non-intersecting surface intertwined with 3d space. TPMS has 2 types such as follows. Sheet Network – Shell like architecture is created with that of characteristics of TPMS maintained on both sides with thickened surface. The volume fraction of re-enforcement phase is controlled by specified thickness. Solid Network – Solidifying one of the partitioned volumes by the TPMS topology which its properties are maintained on the interfere between the two dissimilar co-continuous phases From **Fig.2.1** you can see Interpenetrating Phase Composite (IPC) solid and sheet network structured IPC.

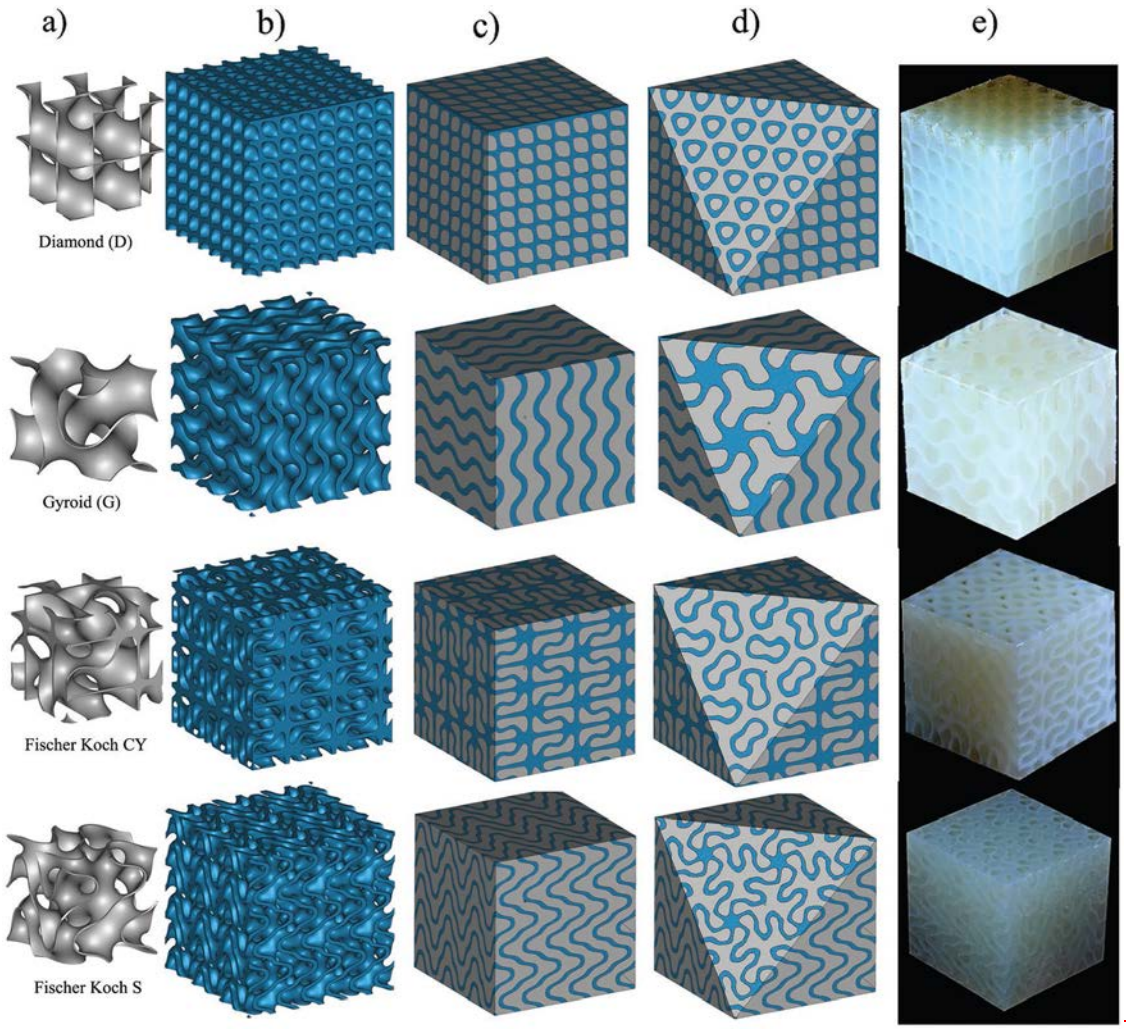

Fig.2.1 – Solid and sheet networks IPC [1]

The advantage of interpenetrating reinforcement structures over the traditional (discrete) reinforcement structure lies in their deformation mechanism. Interpenetrating reinforcement structures are continuous throughout the matrix such that they share the same strain experienced by the matrix and endure higher levels of stress through structural bending, stretching, and/or buckling. Unlike random structures, these can be controlled in periodic structures via controlling the topology and spatial distribution of the phases, providing avenues to tailor a material property to fit a desired application. In IPC, the softer material contributes by absorbing the energy released in cracking events, resulting in arresting cracks from excessive propagation, which prevents catastrophic failure of the harder phase [1]. Diab W. Abueidda at al. [2]reported

good correlation between numerical investigation and experimental data of obtained electrical conductivity of the 3d periodic IPC's in **Fig.2.2**.

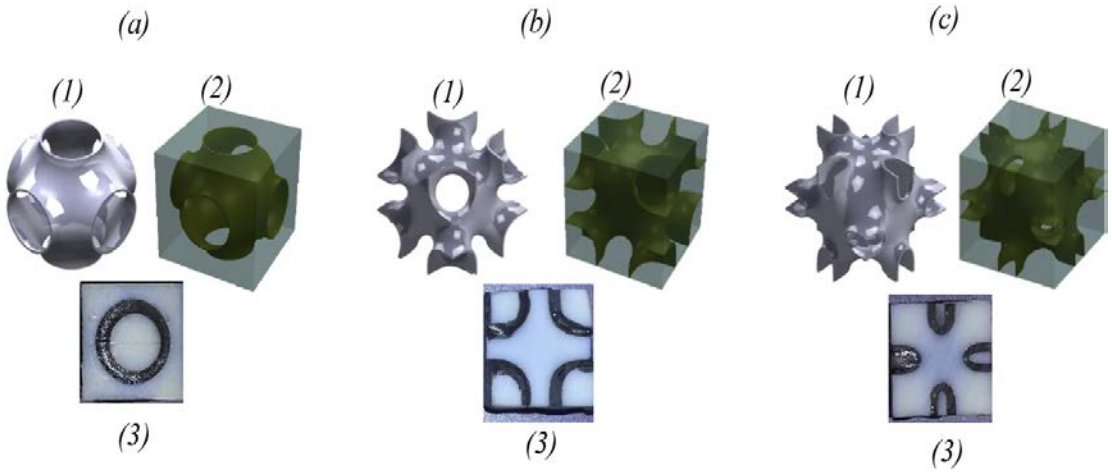

Fig.2.2 – IPC's based on TPMS (a) primitive, (b) Schoen's minimal surface, (c) neovius surface [2]

Summarizing the whole investigation of IPC sheet network re-enforcements has more advantage over solid network and other forms of periodic interpenetrating phase composites with respect to superior stiffness, strength and toughness. Because of intrinsic continuity and interconnectivity this also confines the crack propagation. Sheet network IPC has better energy absorbing mechanism because it's more periodic over the solid network multiphase composites and possibly has potential for further research and application.

There is a lot of investigation on advanced cellular lattice structured materials. As an example, in article [3] author mainly focuses on fabricating of metal cellular structures that could be uniquely classified materials. They can offer high performance features such as high strength accompanied by a relatively low mass and good energy absorption characteristics**.**

In general, there are 2 types of metal cellular structures:

a) stochastic porous structure which has random distribution of open or closed voids in the lattice cellular structure,

b) periodic metal lattice which has uniform structures that are based on repeating unit cells of periodic structures showing much greater strength and stability. Which helps in load sustaining capabilities by controlling structure properties.

Also in article [4], author describes that SLM has unique advantages to manufacture periodic cellular lattice with the same (CAD) design over the other AM technologies. Which is making more complex 3D structure directly and are then post processed with infiltration. Hot isostatic pressing is not required for the printed lattices made by DMLS and SLM. Different unit cell sizes were investigated ranging from 3-7 mm and with a volume fraction 5- 15 % of printed material. Furthermore, DMLS and SLM have not been explored very much regarding variations of parameters like cell size and volume fraction for printing. According to [3], manufacturing of aluminium alloy DMLS was successful for structures with volume fractions 7.5-10% and cell size 3-7mm. This was defined in the investigation by the author how increasing the unit cell size at a constant volume fraction results in decreased number of unit cells with bigger pores and stronger longer structures connecting them. In [4] authors face a problem that unit size cell 1.25, 2.5, 5 mm was problematic to fabricate as the structure within the structure tends to sag during the SLM process. However, in [3] author also was not successful to print these unit cell size with DMLS.

The author further investigates periodic cellular lattice structures with unit cell type called “Schoen Gyroid” also known as Gyroid cellular lattice structure. These gyroid lattice structures are self-supporting that pave way for manufacturing more advanced and construct cellular lattice structures with large unit cell sizes without the need for support structures. In [4] author used 316L steel powder with particle size of 45±10 μm and in [3] it was 140±15 μm.

Moreover, Chunze Yana [3] focused on the influence of unit cell size to failure and to analyse further why it happened. The reason is that consequently very low volume fraction and unit cell size may result in loss of connectivity between adjacent cells or the structures which are too thin to be manufactures by DMLS process (**Fig.2.3)**.

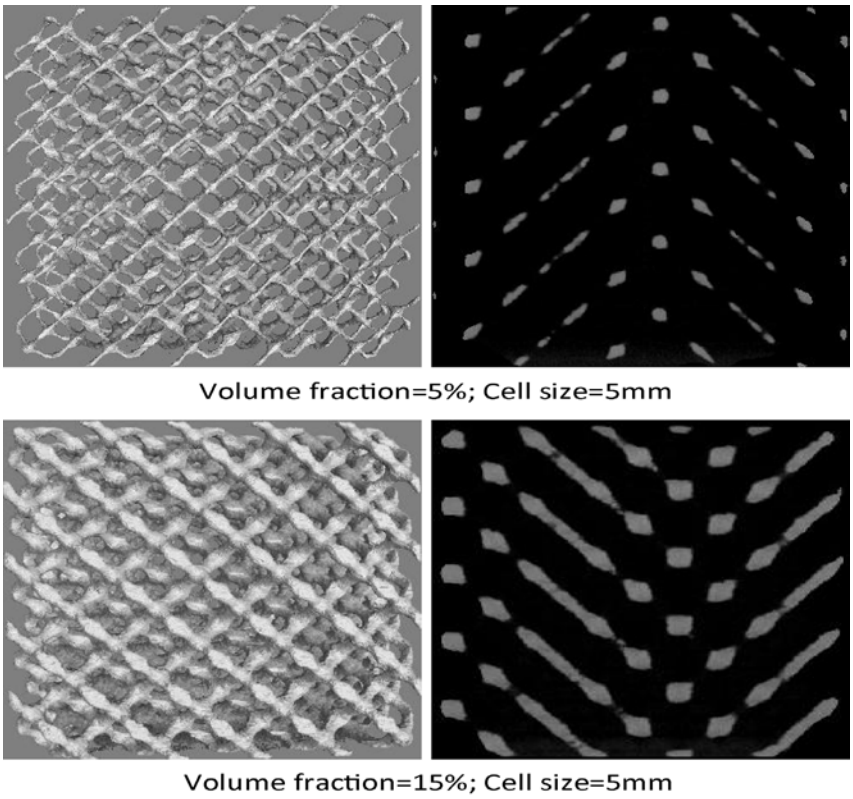

Fig.2.3. Micro-CT reconstruction models and cross section images of the DMLS-manufactured cellular lattice structures at different volume fraction = 5%, cell size = 5 mm, volume fraction = 15%, cell size = 5 mm. [3]

In the case of SLM process there is a critical unit cell size. This depends on the volume fraction of the material. In case of SLM in general the unit cell sizes are much smaller than DMLS.

As analysed in the article [3], the author tried DMLS process using aluminium alloy can be manufactured with only volume fraction of ranging from 7.5 to 15% and unit cell size ranging from (3-7mm). Below the limit (3 to 7mm unit cell size) which author identified as structure and pore sizes both increase with increasing the unit cell sizes at volume fraction as mentioned above. However, with SLM [4] cell size of 2 mm has a relative density of 99.5% which is higher than the relative density of the structure of 8 mm size with relative density of 90.6%. This is also a vital reason which tributes to the shorter scan vector length and better wetting conditions for 316L stainless steel cellular structure during SLM process. Compressive

modulus and strength of the cellular lattice structures with different cell sizes at the same volume fraction indicate that the unit cell size also has an influence on the mechanical properties of the DMLS manufactured samples. In with aluminium lattice structures compressive modulus and strength both decrease with increasing unit cell size. When unit cell size was increased from 3mm to 7mm at a fixed volume fraction of 10% the compressive modulus is reduced from 198.39 MPa to 177.89 MPa (which is 11.5% reduction) and then compressive strength reduced from 10.56 MPa to 7.45 MPa (which is 41.7% reduction). Similar results were observed with 316L stainless steel cellular structures. The cross-section area becomes smaller when unit cell size was decreased and because of this adjacent tracks were scanned more rapidly and therefore continuously leaving less time to cool down in between. Also with 316L yield strength was 3.6% higher for 2 mm unit cell size than 8 mm. Modulus was 27% higher for 8 mm this was because of structure density of the Gyroid lattice decreases with increasing unit cell size.

Comparing studies [3] and [5], similarities of these studies were in the same for DMLS process. Specific volume fractions were varied from (5 to 20%) with unit cell size of (3-7mm). The results showed that compression strength increases with increased volume fraction which is proved by Gibson-Ashby model. When fixing the volume fraction, both compression strength and micro hardness decrease with increased unit cell size. Lattice structures with smaller unit cell size are cooled faster which gives a finer micro structure.

Slightly moving towards Cu stochastic open cellular fabricated by additive manufacturing has considerable potential for novel and multifunctional thermal and electrical managing systems [6]. Electron beam melting (EBM) was used with the objective to fabricate complex monolithic structures and sandwiched to imply wide range of thermal management and electrical conductivity of Cu in Al alloys [6].

This proves that according to the research carried out by the authors in the above papers, varying the volume fraction and unit cell size of the lattice structures has great significance to the quality of the produced cellular materials. It is also crucial to choose the correct type of additive manufacturing.

2.2. Intermetalides and their application

An alloy is a mixture of metals or a mixture of a metal and other elements. [7] An alloy may be a solid solution of metal elements (a single phase) or a mixture of metallic phases (two or more solutions). Intermetallic compounds are alloys with a defined stoichiometry and crystal structure [7]. A binary solid-solid solution would contain two metals while forming a solid – solid solution when the solute is more than the limit of solubility of solvent, then a second arrangement appears distinct apart from the primary solid solution. This secondary arrangement with the primary arrangement is termed as intermetallic compounds.

In intermetallic compounds the binding is metallic between the primary arrangement and ionic in the secondary arrangement leading to different property of inter metallic compounds. The ionic bonding is due to greater difference in elector-negativities between the solute metal and solvent metal [8].

Due to partial ionic bonding the intermetallic compounds are always very hard, brittle and have similar properties to that of ceramic material in terms of their mechanical properties. The intermetallic compounds which have composition similar to that represented by the molecular formula possess high strength, good creep at high temp, high toughness at cryogenic temp and good machinability. Intermetallics possess mechanical properties such as low temperature ductility [9] and high temperature strength. FeAl, Fe_3Al, Ni_3Al and Ni_3Si are some of them.

General Applications of intermetalides [10]

- Structural automotive aerospace
- Magnetic
- Energy storage batteries hydrogen storage
- Heating elements
- Tools and dies
- Furnace hardware
- Corrosion-resistant piping for chemical industries cladding coatings
- Electronic devices

2.2.1. Fe-Al Intermetalides

Iron (Fe) with atomic number 26 is a metal in the first transition series. Natural iron appears in lustrous silvery-grey colour, which oxidizes in air to hydrated iron oxides known as rust. Powders made of iron are widely used in powder metallurgy. Iron powder is formed as a whole from several other iron particles. The particle sizes vary anywhere from 20 μm [11].

Aluminium (Al) with atomic number 13, is a silvery-white, soft, nonmagnetic, ductile metal. Aluminium is remarkable for the metal's low density and its ability to resist corrosion through the phenomenon known as passivation. Aluminium and its alloys are crucial to the aerospace industry and important in transportation and structures such as building facades and window frames [12].

The iron aluminides, FeAl and Fe_3Al are notable for their low cost of fabrication and both corrosion and oxidation resistance. Also FeAl is characterized by good resistance to catalytic coking, carburization, sulfidation and wear, hence FeAl has seen application as transfer rolls for hot rolled steel strip and air deflector for burning high sulphur coal.

The Structural applications for these compounds have been limited by low ambient ductility, due largely to embrittlement by moisture in air. However, several methods to combat environmental embrittlement have been developed. These include control of grain size and shape, use of alloying elements such as Cr for Fe_3Al and B for FeAl, and the application of oxide or copper coatings. These developments, combined with improved creep and impact resistance provided by alloying, have improved the likelihood that monolithic iron aluminides may be utilized for structural applications [13] alternatively, the excellent corrosion and oxidation resistance of iron aluminides suggests their possible usefulness as coatings.

2.3. Technology

As this investigation is completely design oriented we shall discuss about the technology involved in this process of fabricating the lattice cellular structures to form the IPC's through additive manufacturing methodology and SLM technology in particular. This kind of technology is used in high valued industry such as aerospace, automotive, biomedical products etc. which requires precision and more sustainability for its applications.

2.3.1. Additive manufacturing

The term additive manufacturing is the official industry standard term for all applications of rapid prototyping technology. It is defined as the process of joining materials to make objects from 3d model data usually layer upon layer. When compared to convention design, the additive manufacturing has more freedom and control aspects for designers in fabricating for a desired product. Additive manufacturing draws more attention for this great sustainability because it has improved material efficiency, no tools required for manufacturing fashion which in turn reduces the life cycle impacts and greater engineering functionality compared to other manufacturing processes [14]. The principle scheme of AM is shown in **Fig 2.4**.

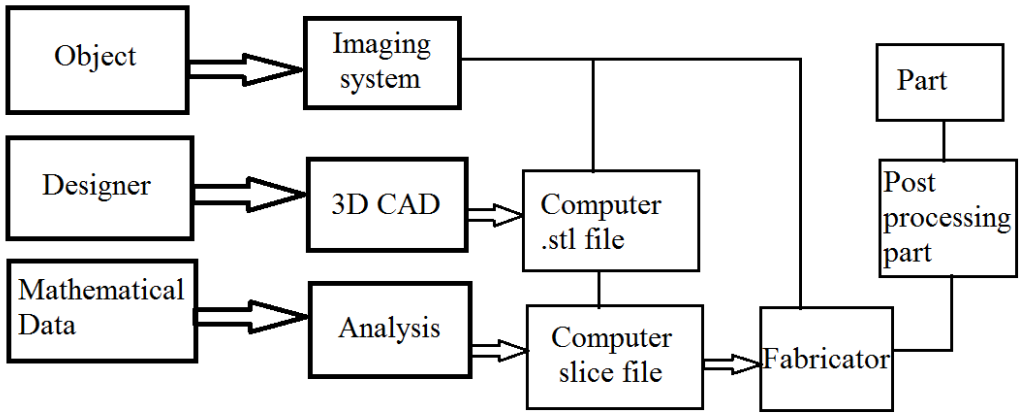

Fig.2.4 – Main process stages common to most additive manufacturing systems

Several types of additive manufacturing process are invented and few have eventually been commercialized. The most popular AM techniques are listed below [15].

- Stereolithography (SLA)
- Fused deposition modelling (FDM)
- Laminated object manufacturing (LOM)
- 3D printing (3DP)
- Selective laser sintering (SLS)

- Selective Laser Melting (SLM)
- Laser engineered net shaping (LENS^{TM})
- Electron beam melting (EBM)

Selective Laser Sintering and Direct Metal Laser Sintering are nothing but the same thing as with SLS used to refer the process and applied to a variety of materials such as plastics, glass and ceramics. Whereas DMLS refers to the process as applied to mostly metal alloys. But what sets sintering from melting is that the sintering processes do not fully melt the powder but heat it to the point that the powder can fuse together on a cellular lattice level and with sintering the porosity of the material can be controlled.

2.3.2. Selective laser melting (SLM)

Selective Laser Melting (SLM) on the other hand can do the same as sintering and go one further by using the laser to achieve a full melt. Which means the powder is not merely fused together but is actually melted into a homogenous structure which makes melting the way to go for a mono material as there's just one melting point and not the variety to find in an alloy. So in common terms SLM is stronger because it has fewer or no voids which helps prevent part failure but is only feasible while using with a single metal powder [16].

The process is as follows building platform covered with a layer of powder corresponding thickness. After scanning laser powder layer platform moves down to the thickness of one layer and the process repeats as shown in **Fig. 2.5**

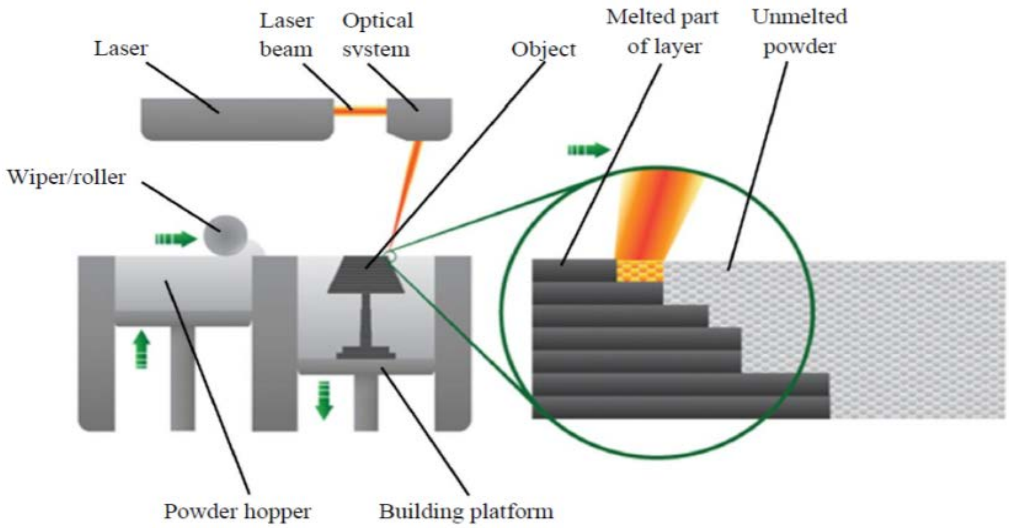

Fig.2.5 – SLM working principle [16]

Each layer in the software is divided into a set of parallel lines each of which in turn consists of a set of discrete points, which are located at a distance from one another. Each layer melted by laser beam point by point line by line (**Fig.2.6**) Distance between points and exposure time are determined scanning speed.

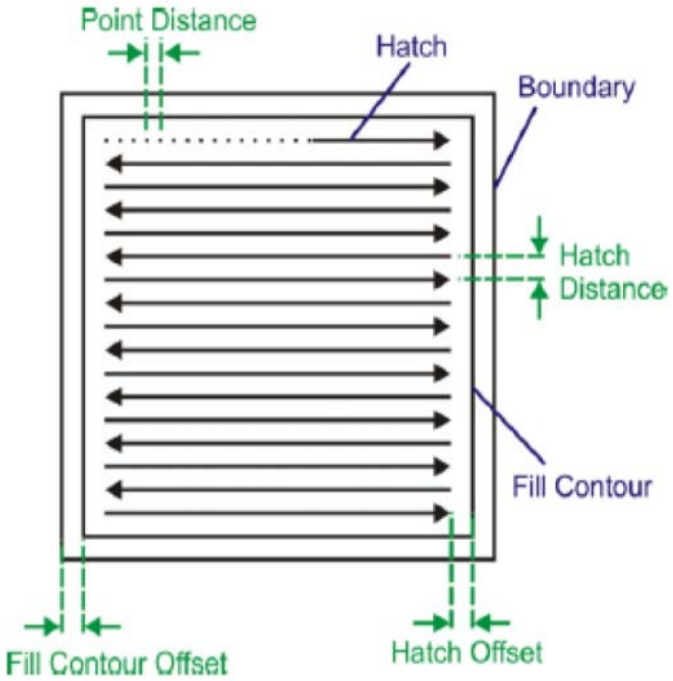

Fig.2.6 – SLM scan mechanism [17]

Vital part of this process is the arc-shaped melt pools overlapping with each other to comprise nearly fully dense structures (≥ 99%) further this is divided into 2 boundary of melt pool has two boundaries one is the zone of heat of the laser direct laser heat and second is the heat affected zone in **Fig.2.7**

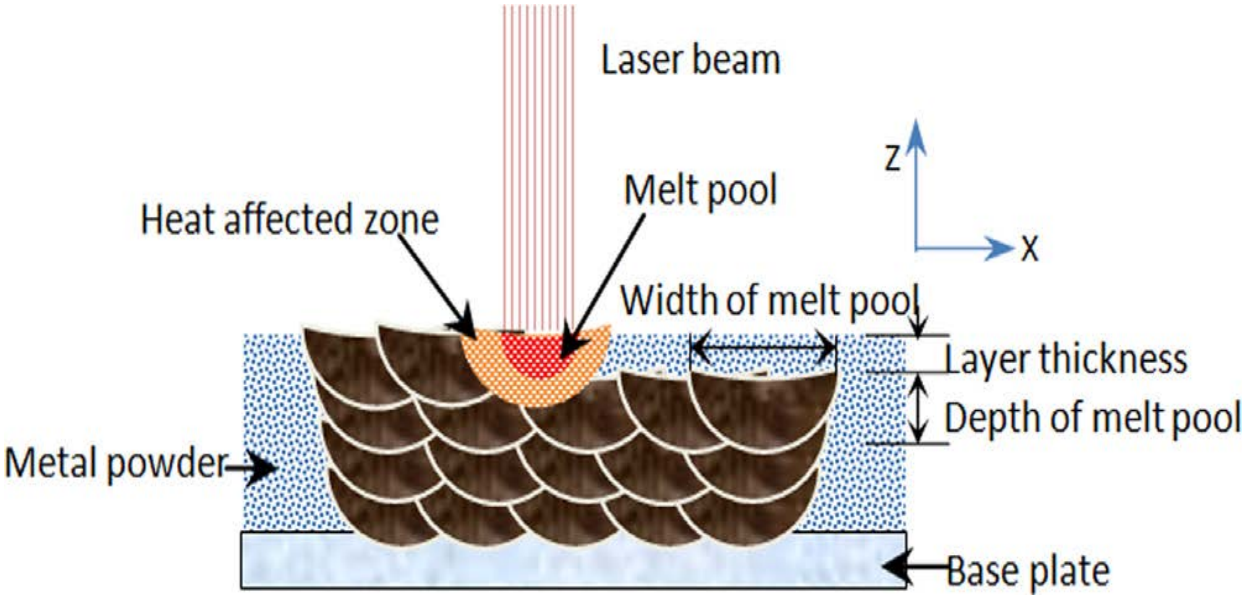

Fig.2.7 - Melt pool formation during SLM process [18]

2.4. Objectives

In present study parameters for selective laser melting of iron powder with particle size less than 90 μm were investigated. The best set SLM parameters was used to obtain periodical iron lattice structures. This lattices were used to obtain inter penetrating phase composite materials by filling it with aluminium by centrifugal casting methodology. Properties of obtained composites are investigated.

3. Experimental
3.1 Raw materials

In the present work two different powders were used such as listed below and SEM scanned images of the raw powders are listed as follows iron powder (a) with 99.7% Iron powder size was up to 90 μm, aluminium powder (b) with 99.7% in **Fig.3.1**.

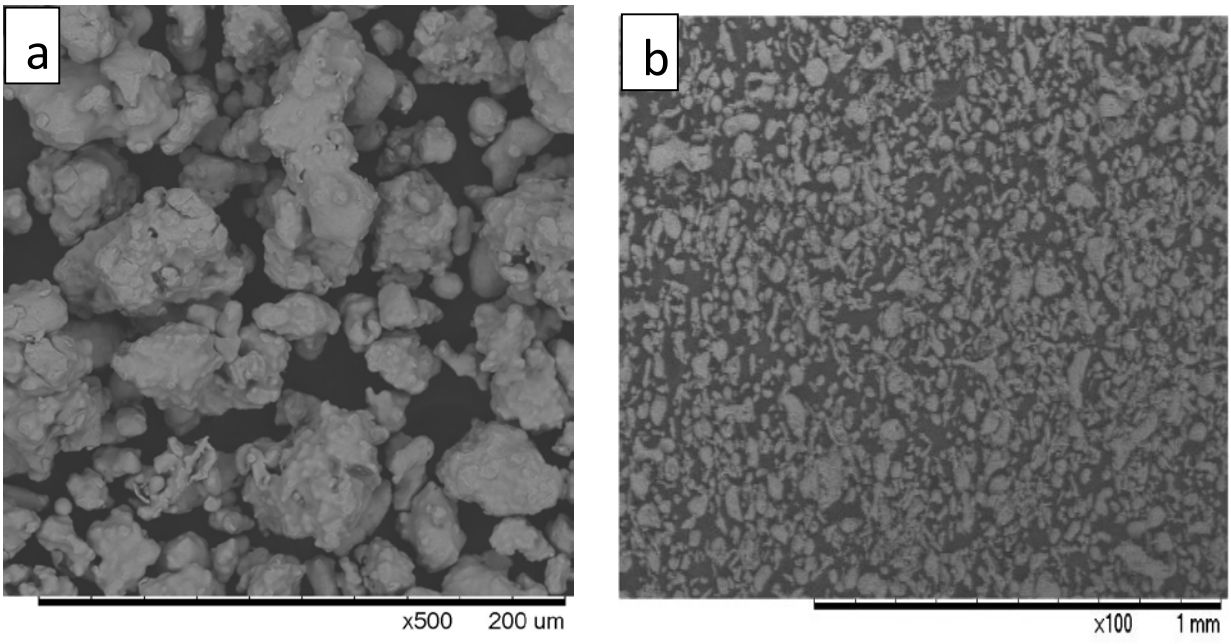

Fig 3.1 - SEM images of the raw powders, iron powder (a), aluminium powder (b)

Schematic technical flow comparison between conventional and additive manufacturing way is presented on **Fig.3.2** Conventional method has raw powder being mixed with pressing and sintering in SPS machine. In additive manufacturing method the same raw powder was used to fabricate porous lattices by the SLM printer, further with embedding porous sample with another material.

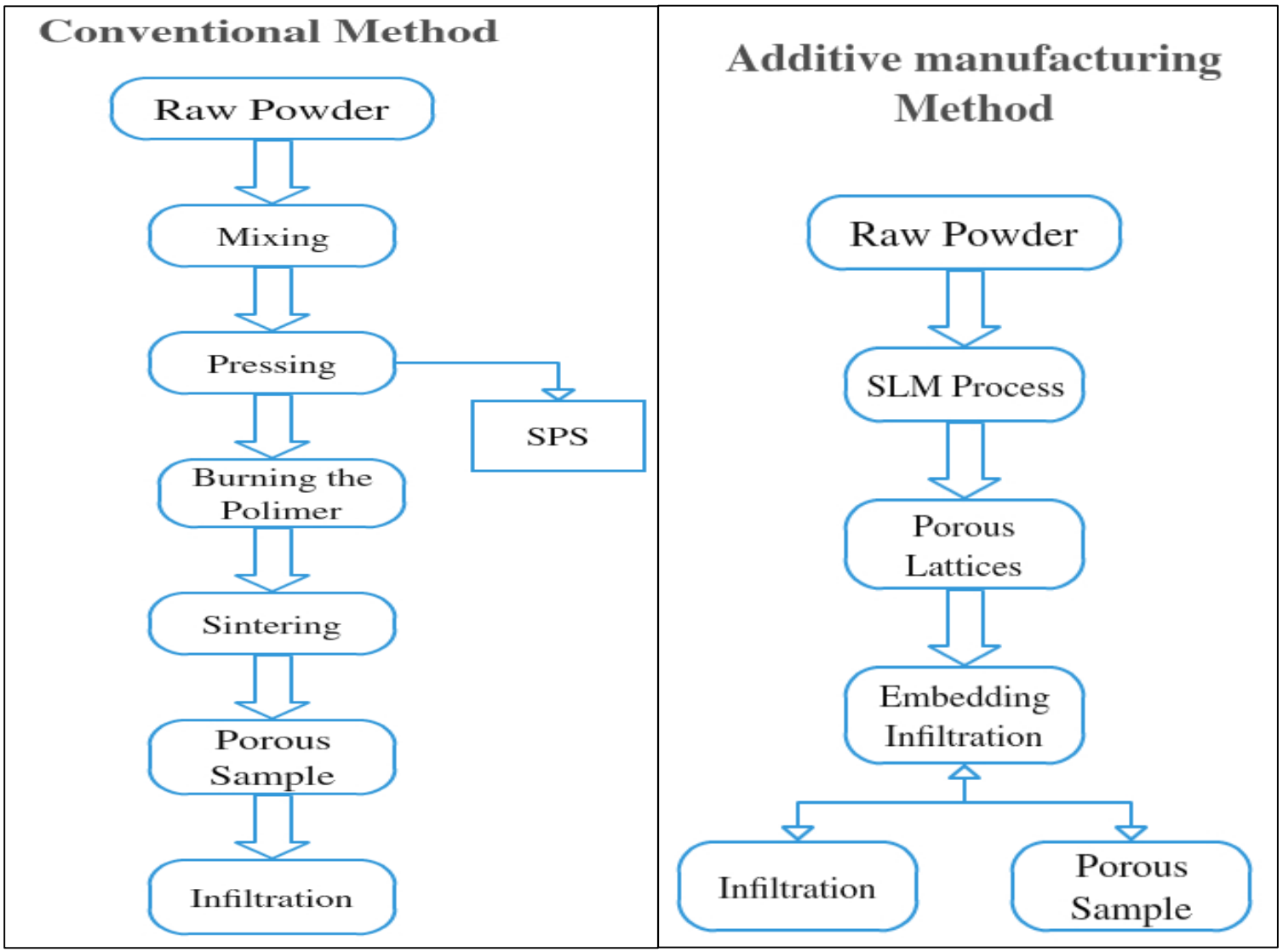

Fig.3.2 Conventional – Technical flow (left) and Additive manufacturing – Technical flow (Right)

3.2 Method

3.2.1Selective Laser Melting (SLM)

In this basic process we use Realizer SLM50 selective laser melting machine. The parameters that can be controlled are laser power, point distance between the focused laser spots, exposure time that it resides at each point and the distance between the laser hatches. The Realizer machine also allows the modification of several other parameters. Also different scanning patterns, scan orientation at each layer and the boundary scanning parameters can be changed. The parameter for obtaining bulk parts from iron powder are listed below

- Exposure time - 50 µs
- Point distance - 20 µm.
- Laser current I= 3000 mA (72 W)

For obtaining lattice structures laser power was 72 W and exposure time was 600 µs. Final strut thickness was defined by combination of laser power and exposure time. Higher ET causes bigger melt pool size and bigger strut diameter. Before printing process 3D model should be sliced and hatched in RDesigner software. The layer thickness was 70 µm. Print can be started only when building platform will be in correct position. Oxygen level in average was less than 0.2%. Argon was used as the protective atmosphere in the chamber.

3.2.2 Spark plasma sintering (SPS)

SPS is a sintering process that allows densification of ceramics and other powdered materials with fast process cycle times (fast heating and cooling). In the SPS furnace pulsed DC current is directly passing through the graphite die as well as the powder compact (**Fig.3.3)**. Die also acts as a heating source and that the sample is heated from both outside and inside is similar to heat generation is internal which is in contrast to the conventional hot pressing by external source. [19] Printed iron lattice structure was filled with Al powder and the resulted sample was placed in the sample holder. Main parameters are as follows: Heating rate of 150°–200°C/min until 600°C as the final sintering temperature (TF) and a holding time of 10 min at this temperature.

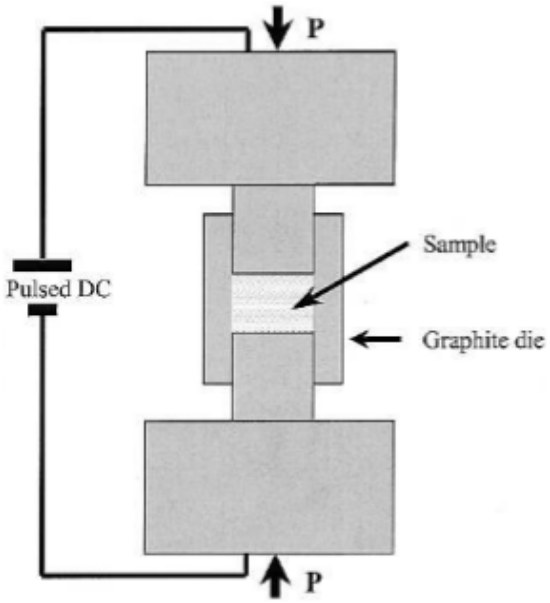

Fig.3.3 – Scheme of SPS [19]

Compacting force of 3 kN was applied from the start and till the end of the holding time the pressure was released. The samples is taken out as shown in **Fig.3.4** below for 1.2 mm unit cell size of iron lattice after polishing.

Fig.3.4 – SLM printed iron lattice SPS sample with aluminium

3.2.3 Sintering and heat treatment

The temperature used for sintering was 650° C which is below the melting point of aluminium which is around 660° C. The samples obtained after SPS sintering were treated with a 2 stage diffusion process in a tube furnace. For obtaining the intermetallide 1st stage is heating it the sample for 4 h under vacuum with 675° C and holding in this temperature for 1 h further. Second stage is increasing the temperature to 975° C [20] and then kept for 1 h.

3.2.4 Centrifugal casting

Centrifugal casting machine operates on basic principle of centrifugal force on a rotating component. In this operation a mould is rotated about its central axis when the molten aluminium is poured into it [21]. A centrifugal force acts on the molten aluminium due to this rotation which forces the aluminium at outer wall of crucible. Melted aluminium flows to the casting mould with the sample in the other chamber of the mould as shown in the **Fig.3.5** in procedure a – centrifugal machine chamber, b – centrifugal machine chamber with crucible, c – with mould and d – removing the mould after process.

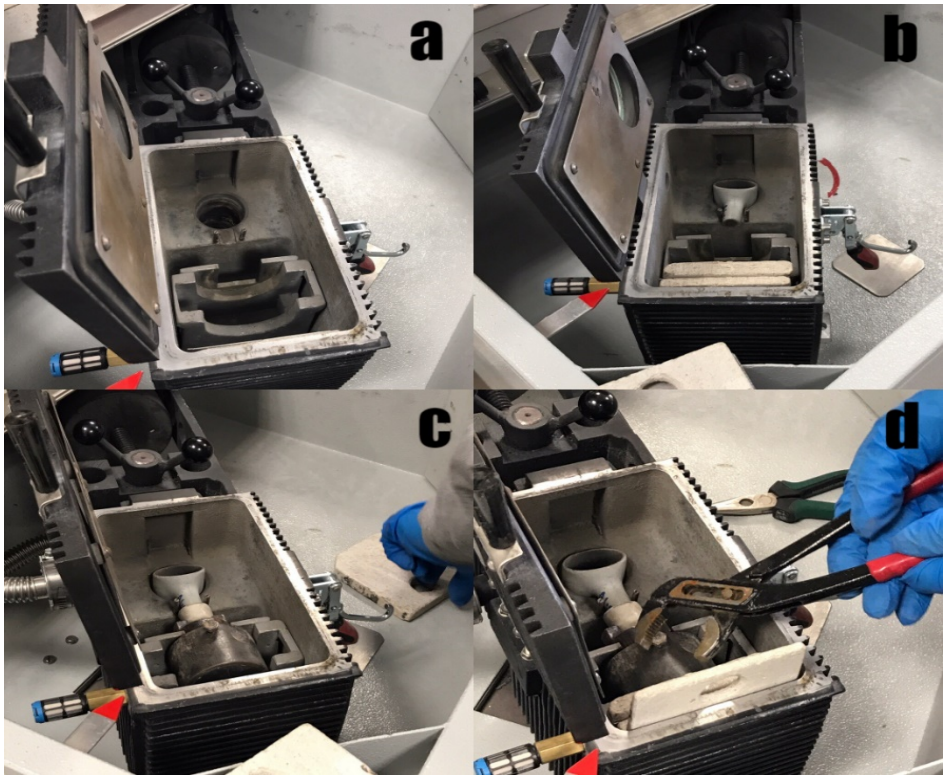

Fig.3.5 – centrifugal process

Fig. 3.6 - Paraffin used as the base

Sample is prepared with placing the printed iron lattice of 0.8 mm, 1 mm, 1.2 mm, 1.4 mm unit cell size in gypsum where the base has to be elevated from the base within the mould. When gypsum is poured and hardened then paraffin is used as the base as shown in **Fig.3.6**. The slag oxide and other inclusion being lighter they get separated from metal and segregate towards the centre. Hence in this process there are several mould cavities connected with a central sprue with radial gates. The mould with lattice inside for centrifugal process with sample 1.2 mm and 1.4 mm unit cell size were preheated to 250 ^{o}C in a furnace for 5 min and then placed in for the operation. The temperature of the process was 900 ± 50 ^{o}C and was controlled by optical pyrometer.

3.2.5 Lattice generation and obtaining

Lattices were created using Realiser RDesigner software. Generated lattice structure consists of connected vectors with zero thickness. Sample generation follows the following steps, first geometry is imported and then the process control file that defines the lattice parameters is applied. Next layer thickness is defined by slicing followed by lattice generation.

The design of the lattice for unit cell you should choose is done by designing the first and last point of each lattice vector fig. 3.8. Thus each new vector will appear in graphical interface. In “Lattice definition” you also have a possibility to change size of unit cell in three directions, x size, y size and z size. (**Fig 3.7**) – Lattice definition to change printing parameters for the lattice chose “Lattice Structure g1” in tree structure and put the parameters in appropriate fields.

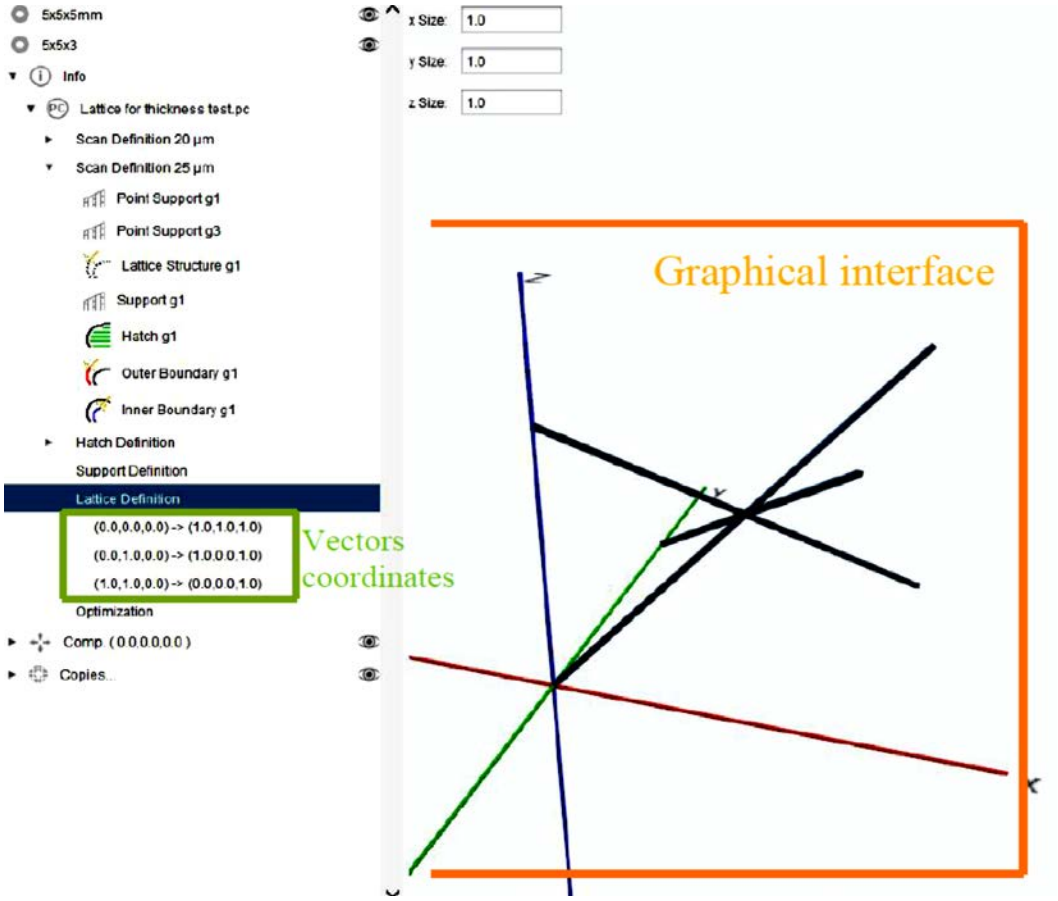

Fig. 3.7 – Lattice definition

3.2.6 Scanning electron microscopy (SEM) and Optical microscopy (OM)

The SEM microscope (SEM) uses a focused beam of high energy electrons generated to variety of signals that surfs over the surface of solid specimens [22]. The signals that derive from electron and sample interactions reveal information on the sample including external morphology, chemical composition and crystalline structure and orientation of materials with horizontal cross section or vertical making up the sample. In this application data is collected over a selected area of the surface of the sample. 2 dimensional image is generated with that displays spatial variations. Also areas ranging from approximately 5 mm to 30 microns in width can be imaged in a scanning mode using Hitachi TM-1000 table top SEM with magnification ranging from 0X to approximately 3000X for spatial resolution of 50 to 100 nm. The SEM is also capable of performing analyses of selected point locations on the sample this approach is

especially useful in qualitatively determining chemical compositions using EDS which we will discuss in the coming chapters. Optical principles the eyepiece is a compound lens which is made of two lenses one near the front and one near the back of the eyepiece tube forming an air separated couplet with a exposure light on the sample to project better image for more analysis [23].

3.2.7 Energy Dispersive X-ray Spectroscopy (EDS)

Energy Dispersive X-ray Spectroscopy (EDS or EDX) is a qualitative and quantitative X-ray micro analytical technique [24] that provides information on the chemical composition of a samples for 45 mass% Fe, 55 mass% Al, SPS EDS. The Characteristic of X-ray generation by the atoms are ionized by the primary electron beam leading to holes generated on the core shells.

Hence following the ionization electrons from outer shells fill the holes and cause the emission of X-ray fluorescence lines and this X-ray lines are named according to the shell in which the initial vacancy occurs and the shell from which an electron drops to fill that vacancy and exalted are analysed.

The results of EDS are presented as shown in table 3.1 and **Fig. 3.8**

Table 3.1 – EDS spectrum

	Matrix			Lattice		
Spectrum	Al	Si	Fe	Al	Si	Fe
Spectrum 1	89.99	9.23	0.79	0.22	0.31	99.47
Spectrum 2	90.45	8.92	0.63	0.21	0.15	99.63
Spectrum 3	90.55	8.75	0.70	0.29	0.51	99.21
Mean	89.99	9.30	0.71	0.24	0.32	99.44

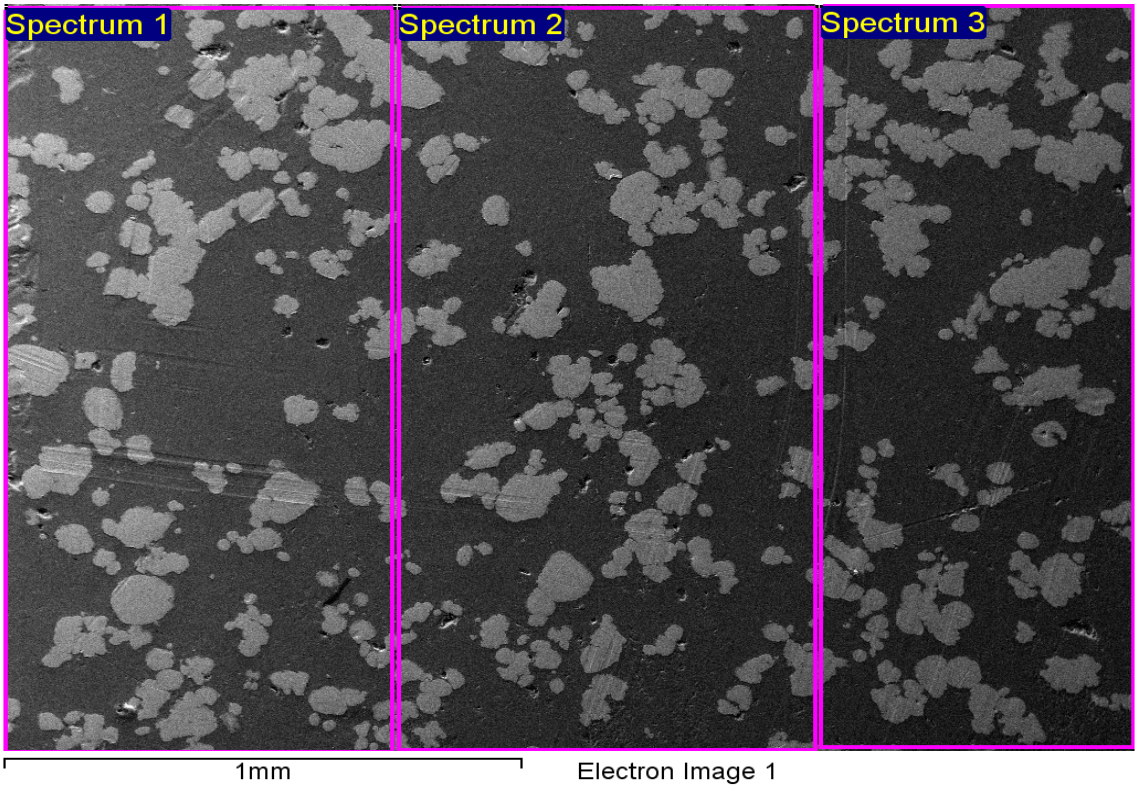

Fig. 3.8 – Places where matrix was analysed

3.2.8 X-ray diffractometry (XRD)

X-ray diffraction (XRD) is a rapid analytical technique that is used for phase identification of a crystalline material and it provides information on unit cell dimensions. These diffracted X-rays are then detected, processed and counted. By scanning the sample through a range of 2θ angles, all possible diffraction directions of the lattice should be attained due to the random orientation of the powdered material.

Conversion of the diffraction peaks to d-spacing's allows identification of the mineral because each mineral has a set of unique d-spacing's [25]. Typically, this is achieved by comparison of d-spacing with standard reference patterns. The analysed material is finely ground, homogenized and average composition is determined as by shown in the **Fig. 3.9**

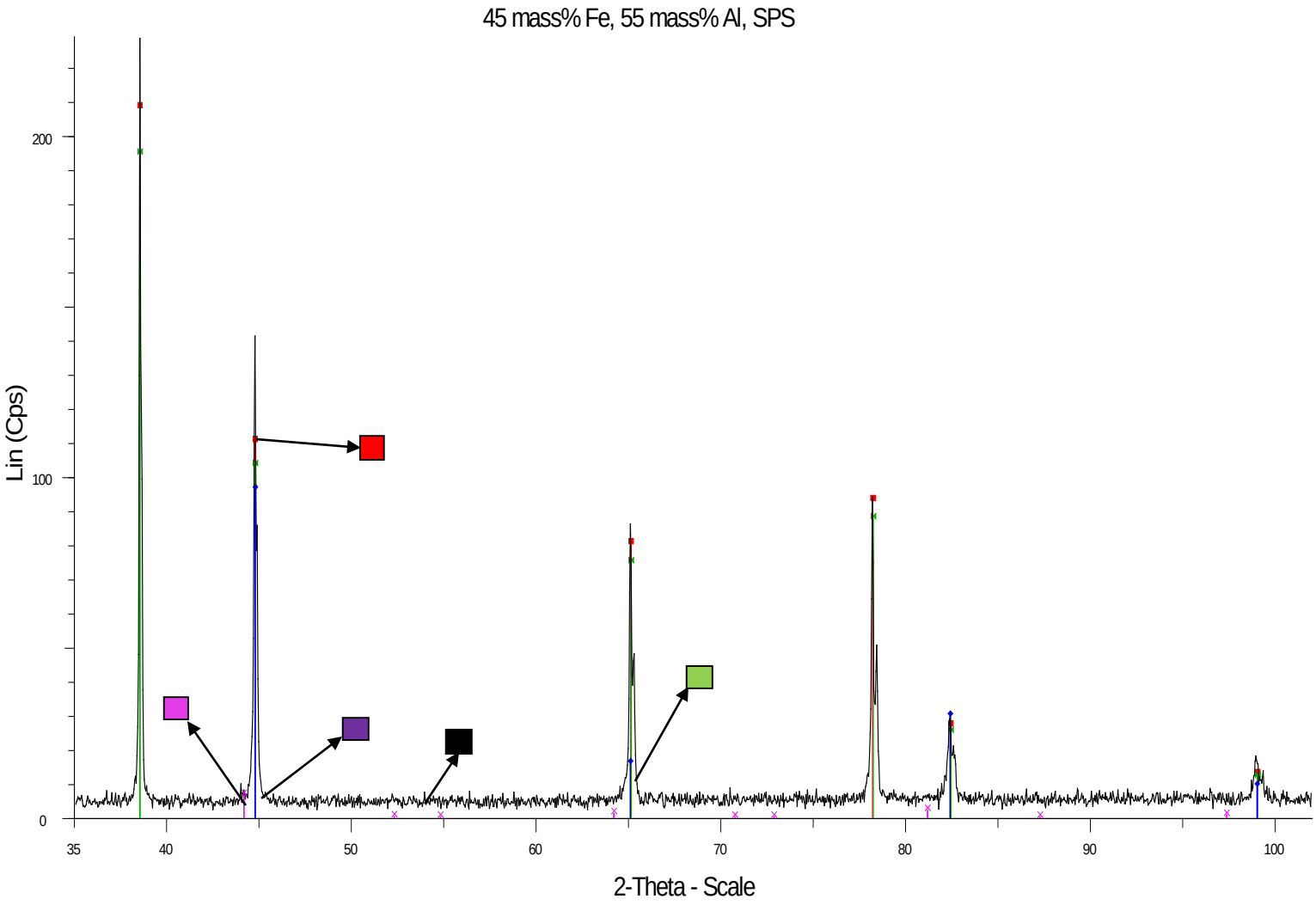

Fig.3.9 – SPS sample Composition

- Al, SPS - File 45 mass % Fe 55 mass%
- Aluminium
- Aluminium and silicon
- Iron- Fe
- Aluminium Iron - Fe3Al

3.2.9 Density measurements

The density is the volumetric mass density of a substance. It is calculated in general as mass per unit volume. The symbol used for density is where ρ, m is the mass, and V is the volume.

$\rho = m / V$

Relative density is defined as the ratio of the density (mass of a unit volume) of a substance to the density of a given reference material. Volume fraction is calculated as below formulae where ρ lattice is the density of the lattice and ρ iron density of the iron.

$$VF = \frac{\rho_{lattice}}{\rho_{iron}}$$

3.2.10 Compression strength measurements

Compressive strength is the capacity of a material or structure to withstand loads tending to reduce the size as opposed to tensile strength. Compressive strength was measured using Instron 8516 servo hydraulic testing system (**Fig. 3.10**). Testing speed was 1 mm/min as shown in the table 3.2 result of compressive test were shown in the table 3.2

Table 3.2 - Compressive maximum stress and yield strength values

Unit cell size (mm)	Compressive max stress (MPa)	Yield strength (MPa)
0.8	121.6	54.6
1	249.9	117.3
1.2	195.5	71.7
1.4	209.1	95

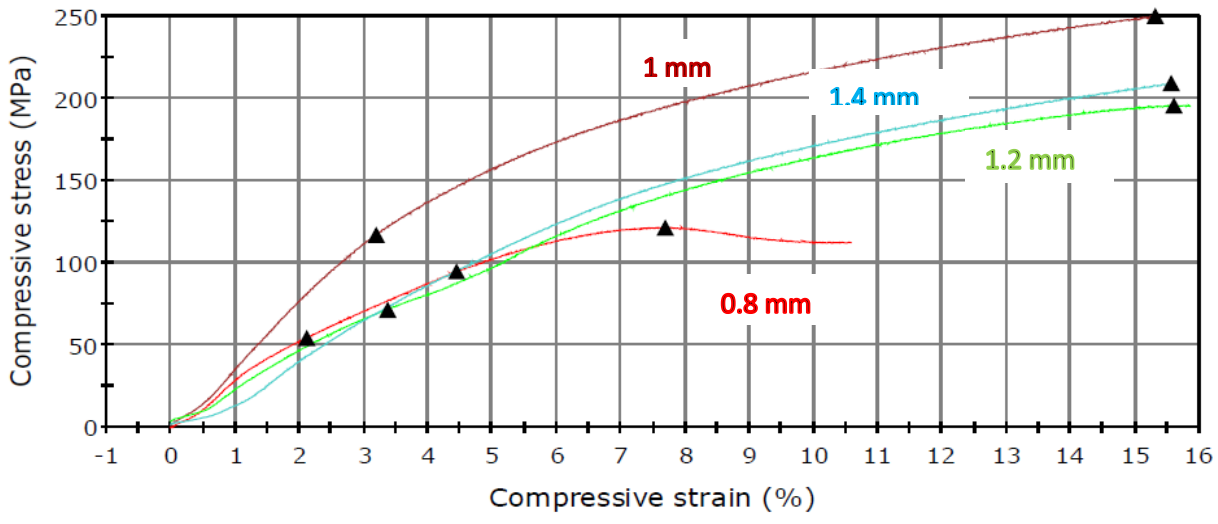

Fig.3.10 – Compressive maximum stress and yield strength values

3.2.11 Vickers hardness measurements

The Vickers hardness test method is based on an optical measurement system. The Micro hardness test procedure specifies a range of loads set using a diamond indenter [26] to make an indentation which is measured and converted to a hardness value. Typically loads from 25 g, 50, 100 etc to 1 kg. Testing the centrifugal Fe-Al casted for 1 mm lattice cellular structure was performed with load 100 g. Measurements were performed only at sample with lattice unit cell size 1 mm. The measured values of hardness of two phases from the sample reinforced by lattice with 1 mm unit cell size is shown in table 3.3

Table 3.3 – Hardness values

No.	Fe	Al
1	122	36.8
2	143	42.6
3	147	46.7
4	147	35.8
5	139	38.9
6	139	34.8
7	131	41.3
8	143	40.1
9	160	41.3
10	147	34.8

4. Results and Discussion

4.1.SLM parameters optimization

This study evaluates the manufacture ability and performance of Fe-Al Architected Interpenetrating Composite materials manufactured by combination of SLM with other methods. In the present study we tried to obtain parts from casual atomized iron powder with near spherical shape with particle size distribution less than 90 µm. That's why process parameters should be optimized with preliminary tests. This study evaluates the manufacture ability and performance of Fe-Al Architected Interpenetrating Composite materials manufactured by combination of SLM with other methods. The lattice structures were designed with the unit cell sizes of 0.8 mm, 1 mm, 1.2 mm, 1.4 mm and 1.6 mm. One of the most important parameters to optimize is layer thickness. It influenced quality, and mechanical

properties of the part as well as speed of SLM process and, as a result, total production time. To find optimal layer thickness for printing non-standardized for additive manufacturing iron powder layer thicknesses of 35 µm 50 µm, 70 µm and 75 µm were used. Usual process of powder layer treating during SLM process is shown in **Fig.4.1**.

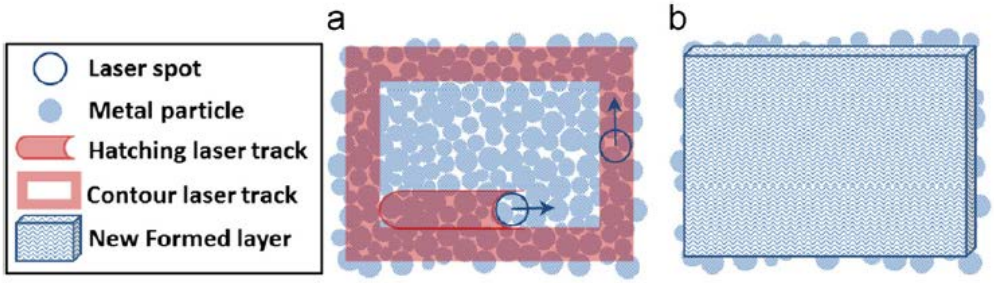

Fig. 4.1 – Powder layer optimal process (a is ongoing, b is finished)

Attempts to obtain lattices and bulk parts with layer thicknesses 35 µm and 50 µm were unsuccessful. At some point of printing job parts started "growing" above the distributed powder layer (**Fig 4.2**). This defect damages the wiper rubber, and if the job would not be stooped in time, parts will grow to critical height and wiper will stuck in the middle of the building platform.

Fig.4.2 – Part growing phenomenon

Usually powder particles size is smaller than layer thickness (**Fig 4.3**). But, when layer thickness is smaller than powder particles size [27], parts are starting to grow. There is more

material on the platform that needed for one layer, that's why solidified part is a bit higher in size. With each new layer this extra height is increasing. During wiper moving free powder on the platform can be rearranged, but solid part is strongly connected to the platform and at some critical point when height of the solid part is big enough, wiper stuck.

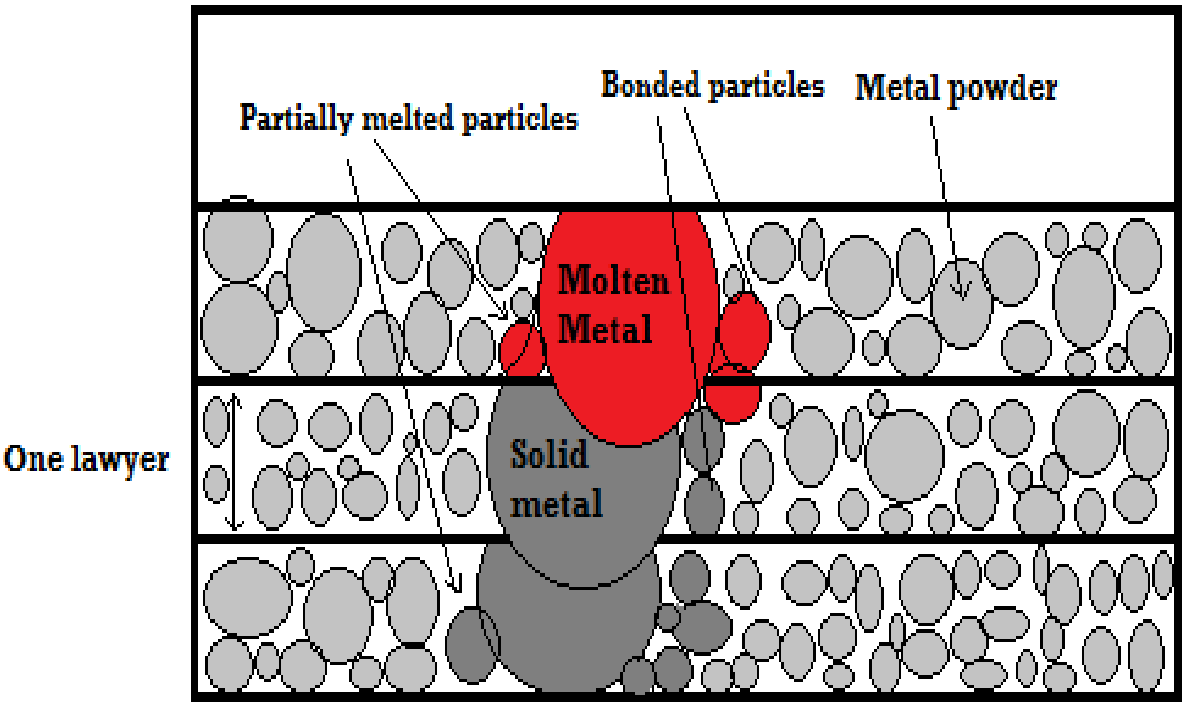

Fig. 4.3 - Scheme of laser melting with normal powder size

With layer thickness 70 and 75 μm these problems disappeared. In spite of the fact that the biggest powder particles have size of 90 μm parts didn't grow any more. The reason behind this is that in the powder are also particles with smaller sizes. Also there is some space in freely distributed powder among particles which is filling during layer melting, and this causes some shrinkage. So, extra volume of material from the particles with 90 μm in size can be distributed to balance the shrinkage during melting.

The optimal layer thickness for present powder was chosen 70 μm. Lattices with different unit cell sizes, obtained at 70 μm layer thickness are shown in **Fig.4.4**

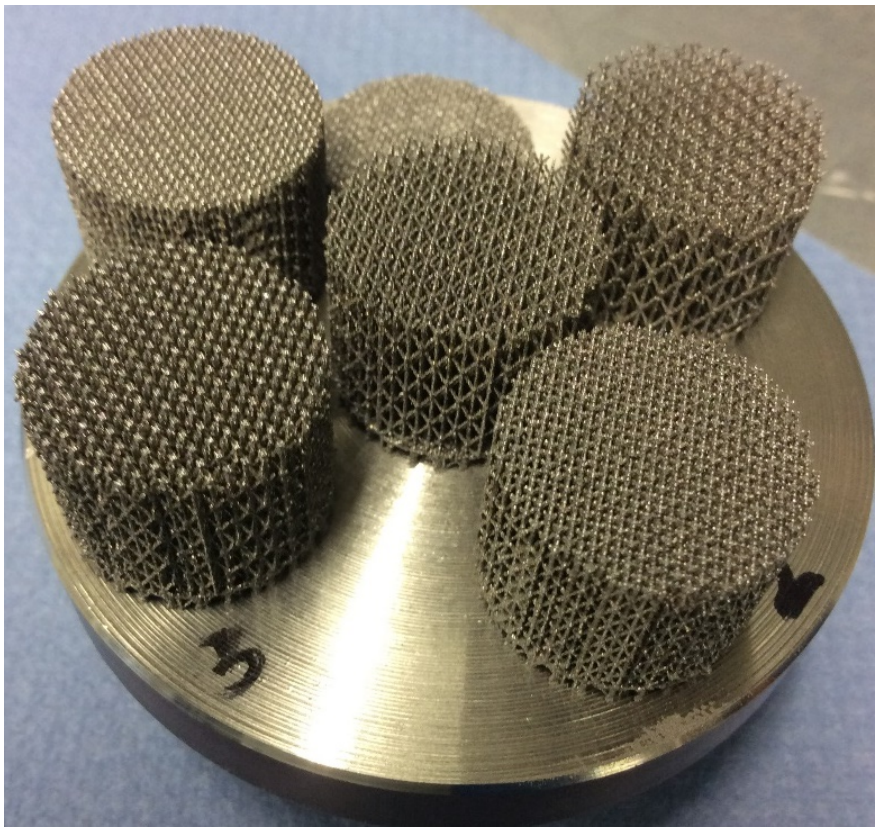

Fig.4.4 – General view of Lattice for SPS obtained with 70 μm

4.2. Iron lattice properties investigation

These complex and novel lattice structures which are very difficult or, in the most cases, even impossible to be produced by conventional manufacturing methods could be made out of metals by SLM. SLM technology and additive manufacturing approach should allow future development of even more advanced and functional cellular lattice structures.

SEM images of iron lattice structures with unit cell size 0.8 and 1.6 mm are presented in **Fig 4.5**. As examined the samples in the SEM we got to observe that strut surfaces are covered with bonded particles. Bonded particles shape and size are the same as initial powder particles. One more feature which could be clearly observed is spherically-shaped sections along the strut. Each spherical section is connected to the previous one. Such phenomenon appeared due to increasing layer thickness up to 70 μm. When the laser is treating one point during certain exposure time local melt pool appears. However, due to surface tension and big layer thickness this melt pool gets spherical-like shape. Big layer thickness and spherical-like shape of melt pool in each layer cause smaller re-melted area on the previous layer and as a result weaker

connection between two neighboring layers. This phenomenon is influencing mechanical properties, because strength of the whole lattice is strongly depends on the elements strength.

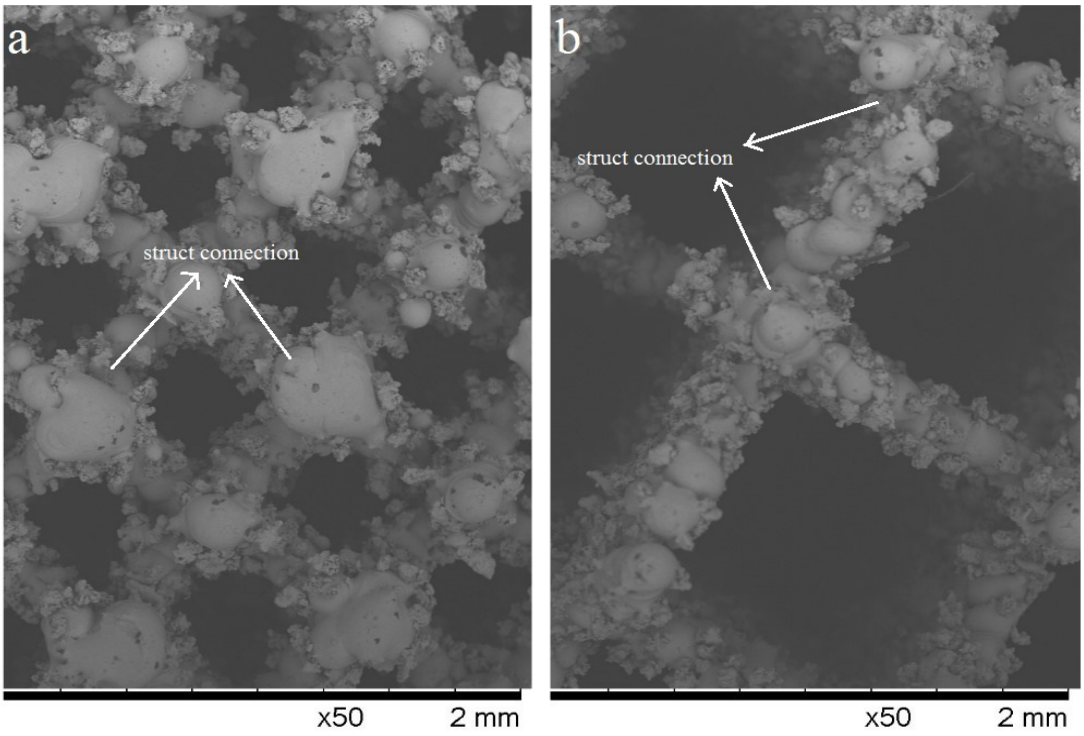

Fig.4.5 – Strut connection a is 0.8mm and b is 1.6mm

Fig.4.6 represents the relative density of the lattice structures with the unit cell sizes 0.8 mm, 1 mm, 1.2 mm, and 1.4 mm. As visible from the graph, increase in unit cell size decreases the relative density of the sample.

Table 4.1 – Relative density and Yield strength of lattices with different unit cell sizes

Unit cell size (mm)	Volume fraction (%)	Yield strength (MPa)
0.8	28.6	27.8
1	20.3	10.6
1.2	14.8	5.9
1.4	11.5	2.9
1.6	9.1	2.2

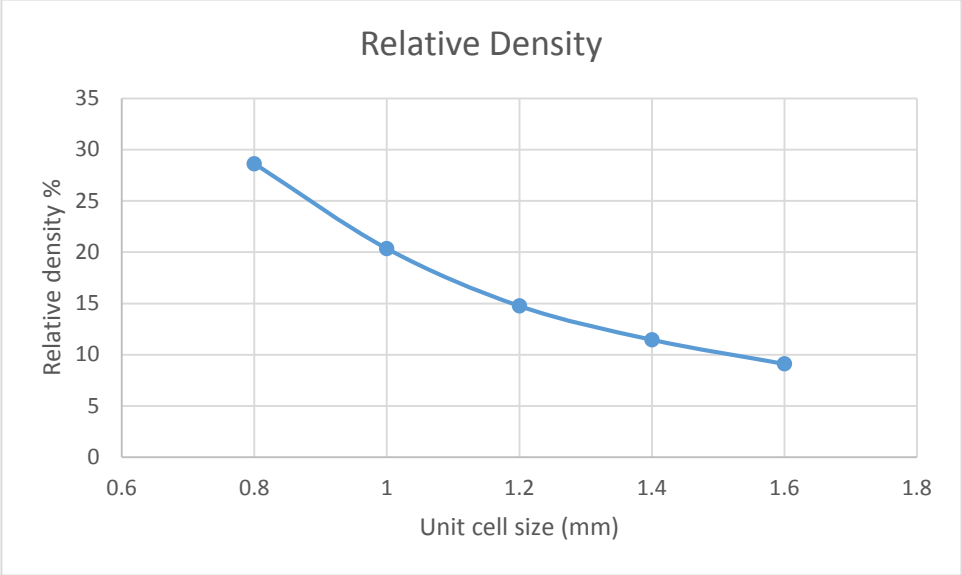

Fig.4.6 – Relative density from unit cell size dependence.

Unit cell size is increased and the number of unit cells in the lattice structures with the same volume decreases. The struts become longer the length of overhangs in the structures increases and it could cause some deformation of the struts during the manufacturing

Yield strength from unit cell size dependence is presented on the **Fig.4.7**. Strength decreases with unit cell size increasing [28].

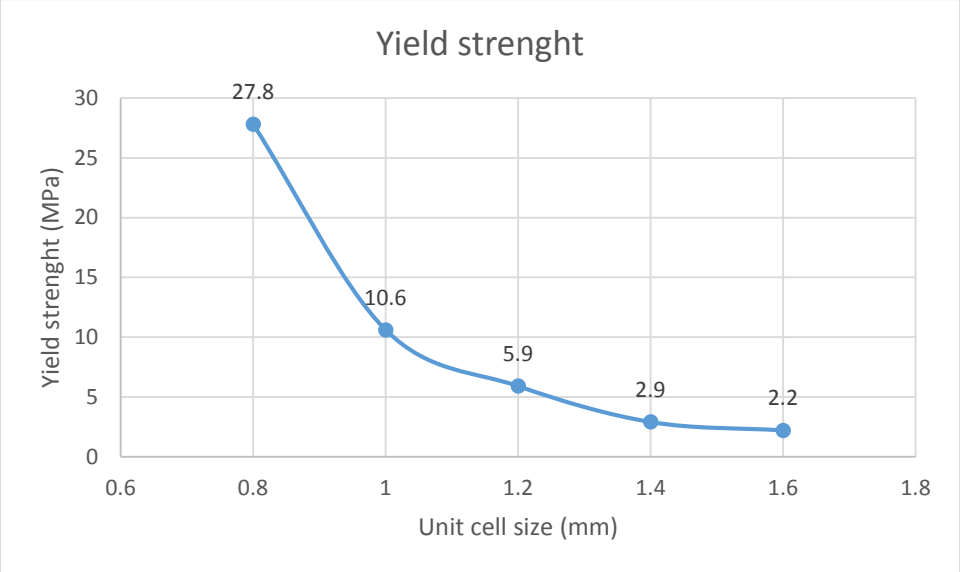

Fig.4.7 – Unit cell dependence on Yield strength

Lattice structures with different unit cell sizes after compressive test and initial ones are presented on in the Fig. 4.8. As visible from the picture unit cell size is influencing not only strength values but also deformation mechanism. For example lattice with unit cell size 0.8 mm, the strongest one, is deforming in the middle of the sample (**Fig 4.8 a**). For unit cell size 1 mm we can observe deformation of the lattice with some unit cells destroying on the top (**Fig 4.8 b**). When starting from unit cell size 1.2 mm till 1.6 mm top layers of lattice structure were destroying „floor by floor“ when other, bottom, part of the rest structure was not damaged or deformed (**Fig 4.8 c-e**). Testing of the sample shown in the **Fig. 4.8 c** was stopped after first lattice layer was destroyed.

Such phenomenon caused by iron plasticity in combination with a high porosity of the structure. Potentially, the behavior of the structure can be applied as an energy absorber for example against impact. Practical application for such materials could be found in the automotive industry to increase safety of transportation in case of accidents. Further investigations in this direction could be done

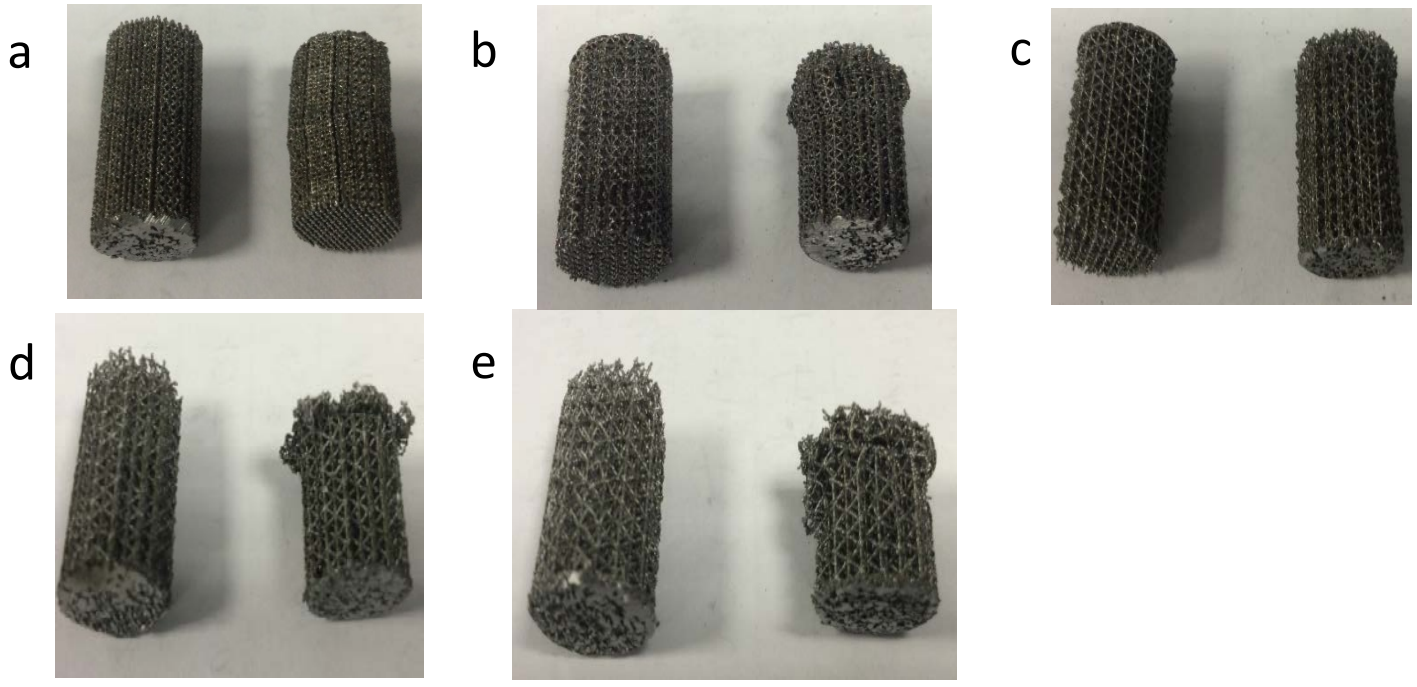

Fig.4.8 – Deformation of Iron lattices with unit cell size 0.8mm (a), 1mm (b), 1.2mm (c), 1.4mm (d), 1.6mm (e)

4.3.Fe-Al Architected Interpenetrating Composite materials properties investigation

Architectured Interpenetrating Composite materials were produced by various methods. First of all, to test SPS regimes and interaction between Al and Fe, sample from Al-Fe mixture was prepared. In the **Fig.4.9** shows structure of the SPS sample obtained out of Al-Fe powder mixture. There are two phases' visible aluminium matrix (dark gray) and iron (light gray). Distributions of the phases are uneven. Average size of iron inclusions is about 70 – 90 μm.

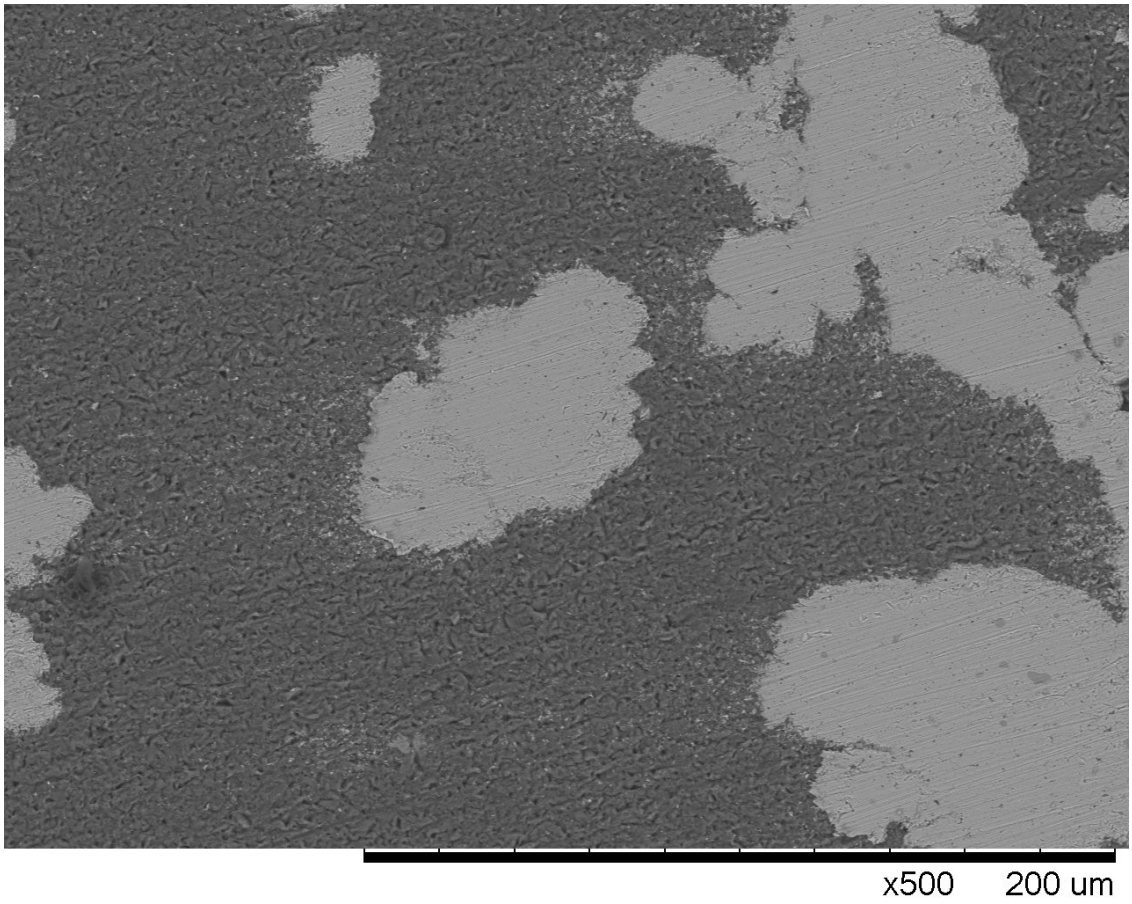

Fig.4.9 - SPS sample obtained out of Al-Fe powder mixture

Fig.4.10 is representing microstructure of the sample obtained with SPS and reinforced with the lattice. There are two phases visible, aluminium matrix (dark gray) and iron lattice (light gray). However, on the interphase boundaries the third phase (middle gray) is present.

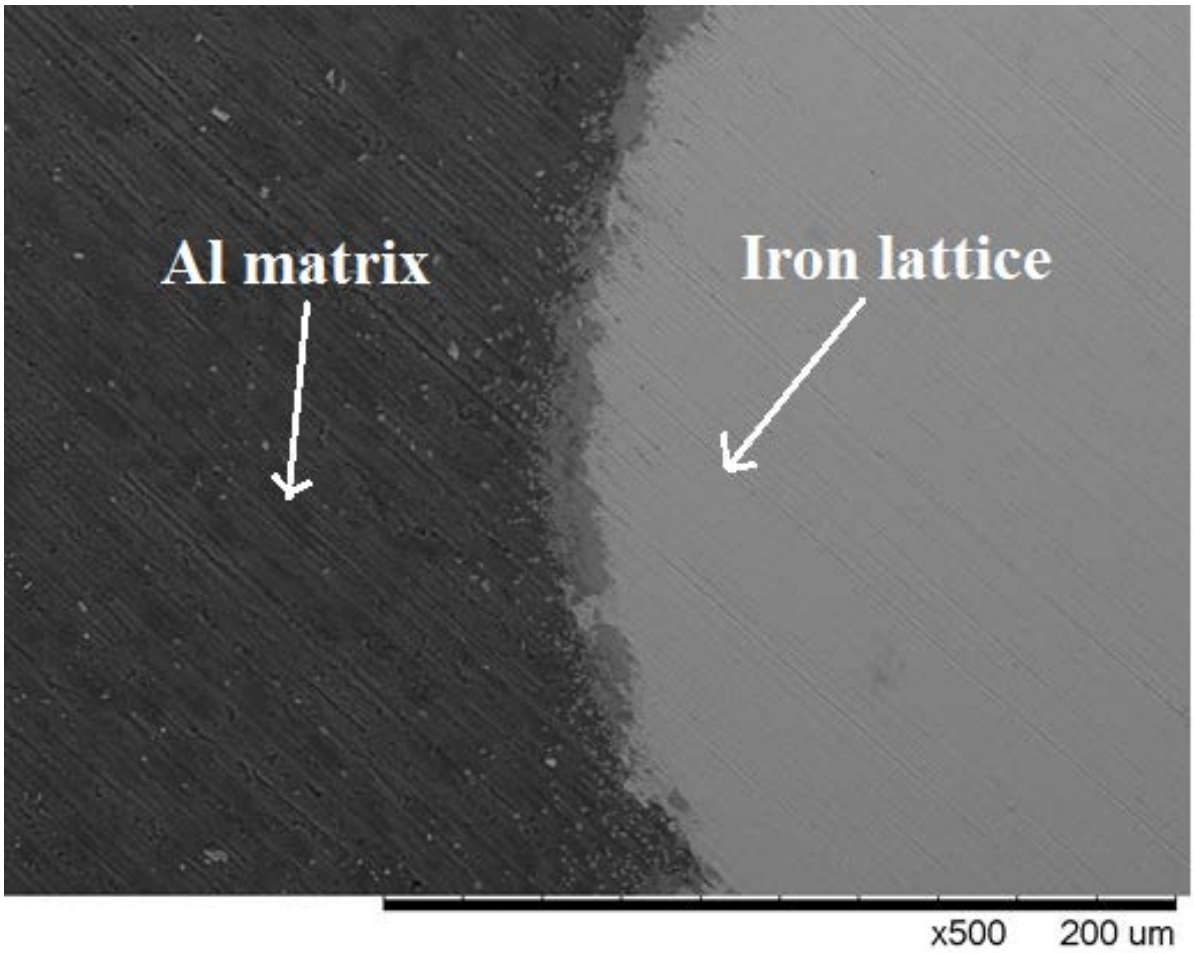

Fig.4.10 - SPS Interphase between lattice and Aluminium (SEM)

But, after etching (**Fig.4.11**), some gaps appeared on the interphase boundaries in the same places where third phase was located before. It is possible that the third phase is just mechanical mixture of iron and aluminium micro-particles. These micro-particles appeared during polishing process and filled the existed gaps near lattice structure. But the particles were removed by etching. Or it could be result of chemical reaction between iron and aluminium, which has low resistance to aggressive environment [29].

Independently from the reason, existing of such gaps, could be an evidence of bad interaction between matrix and reinforcement materials. To improve this surface of the lattice should be modified, parameters or materials should be changed.

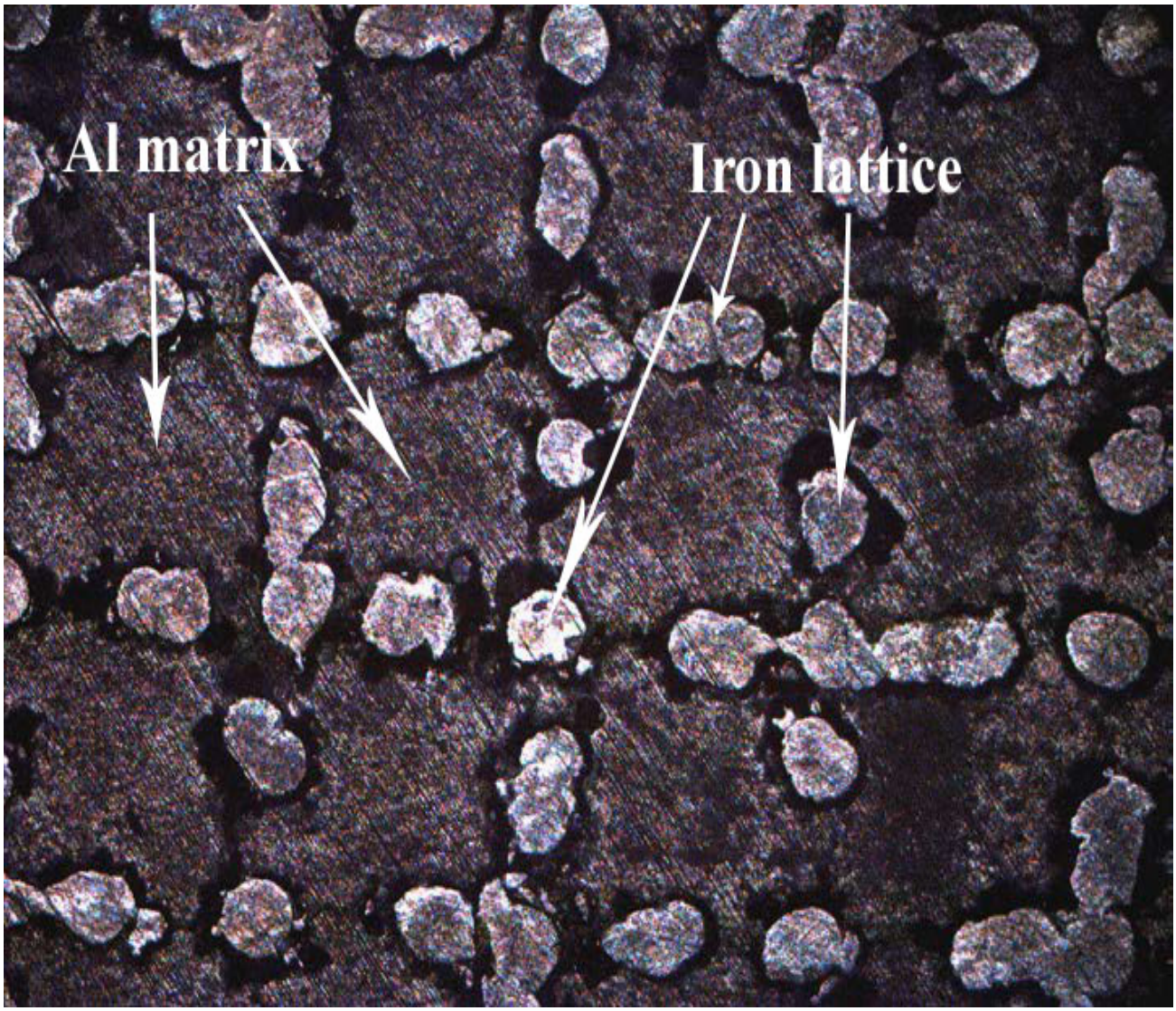

Fig.4.11 - SPS after etching. (OM image)

The **Fig.4.12** shows SEM pictures of lattice samples with impregnated aluminium by centrifugal casting. Preheating of the moulds with lattices to 250 °C was done. Preheating was performed to improve the infiltration by avoiding alloy solidification at too early stage. This sample has some defects near the interphase iron lattice – aluminium alloy boundary.

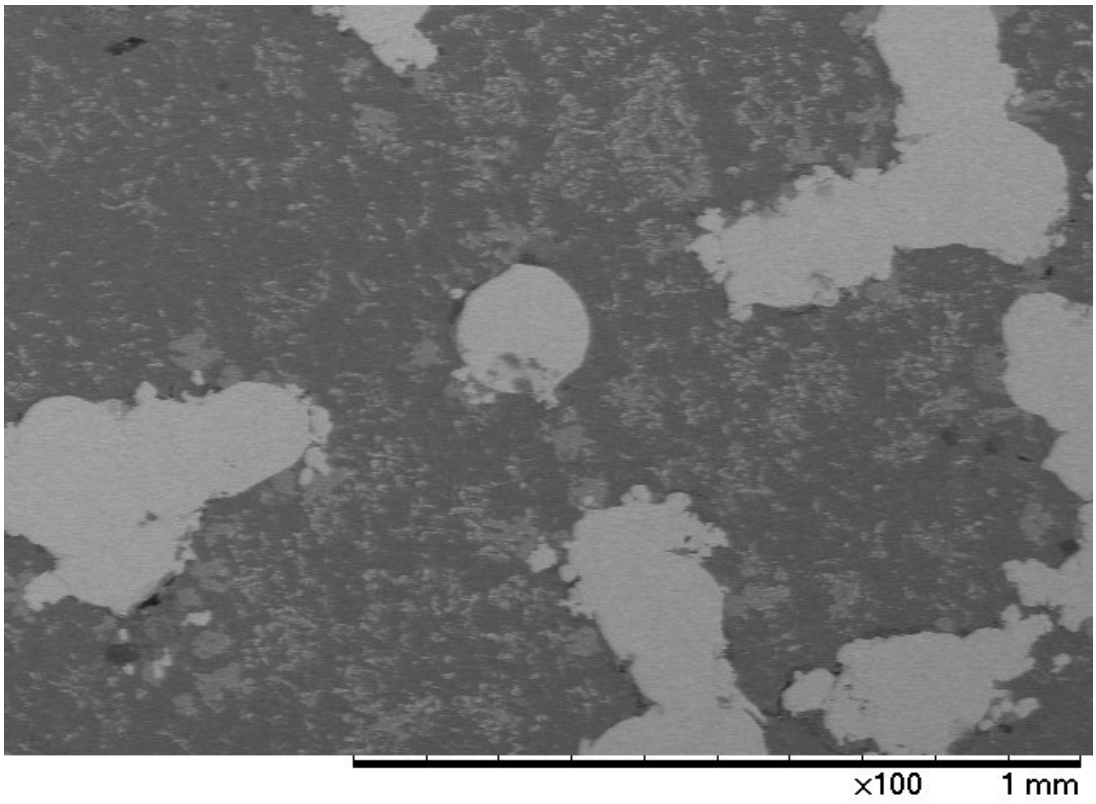

Fig.4.12 - Lattice with impregnated aluminium by centrifugal casting

Intermetalides transformation was not observed in the samples. Hence samples were post processed with 2 stage heat reaction. According to the article [30] which should take place at certain temperature. Since we got less percentage of intermetalides. 2 stage heat reaction for sample was carried out as explained in experimental section for 3.2.3. Experiment was conducted for SPS sample obtained from powder mixture first one in the **Fig.4.13** (a) and SPS sample reinforced by lattice with unit cell size 0.8 mm (b).

Samples were treated for 4 hrs. under vacuum. First stage was performed at 675 C with holding time in this temperature 1 hr. Further second stage is increasing the temperature to 975 C and then kept holding for 1 h and thereafter to cool down. The sample without lattice was destroyed after the reaction. The shape of the sample changed, and it general view was like foam in (**Fig.4.13 (a)**). Might be this happened because the reaction was too fast.

Sample reinforced with lattice has better shape (**Fig.4.13 (b)**) after process. However, some distortion as well as negative shrinkage took place.

The result proves that at elevated temperatures iron aluminide is forming by very active chemical reaction, but during the SPS process forming of intermetalide, probably, was limited by the process temperature 550 C. Reaching higher temperature was too risky, because we couldn't rise the temperature more than Al melting point. Otherwise molten Al would flow out of the mould. Second attempt of post processing was performed at lower heating speeds, but the result was the same – foam was formed.

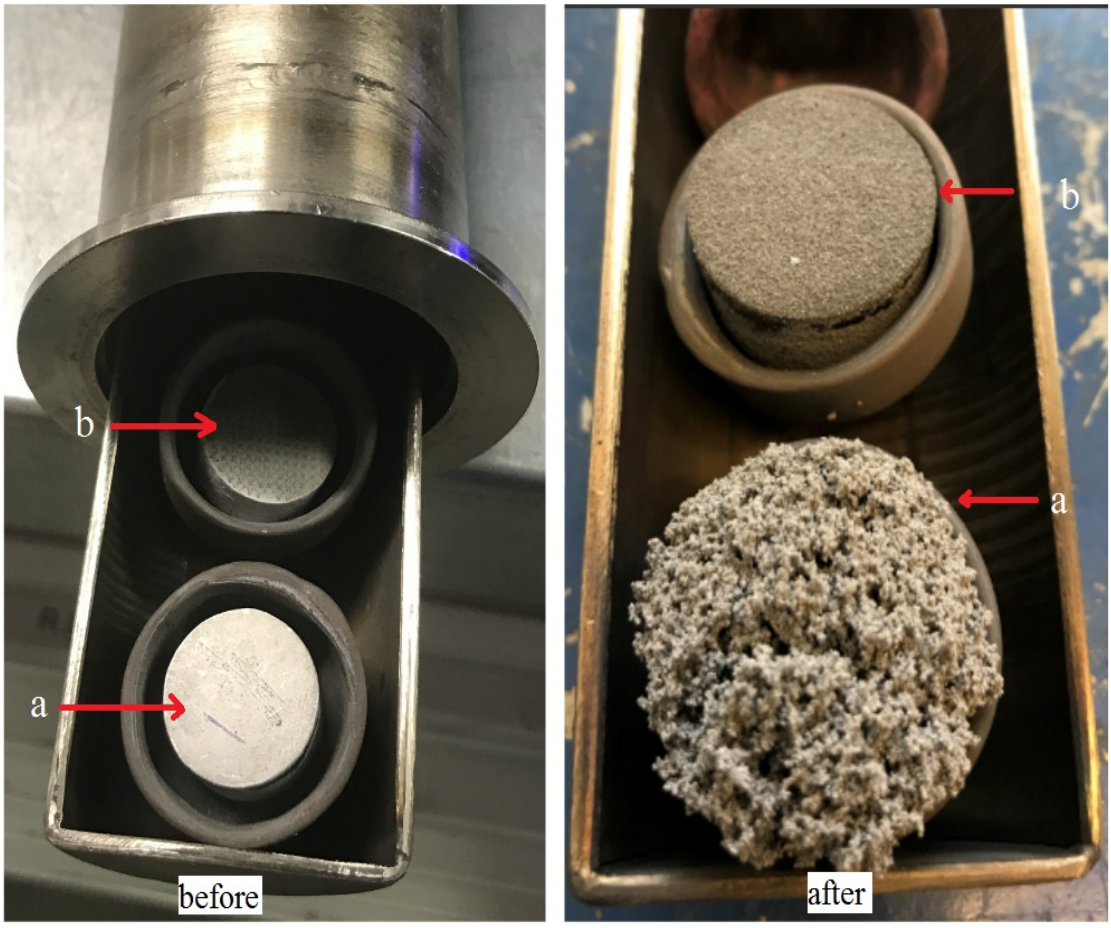

Fig. 4.13 – Post-processing in the furnace for SPS samples

After embedding of iron lattices with aluminium alloy AlSi7Mg, strength values increased 4, 8, 11 and 22 times for samples with unit cell size 0.8 mm, 1 mm 1.2 mm and 1.4 mm respectively. Which is indicates in the below in **Fig.4.14**

The base red line is for the yield strength of reference aluminium alloy sample. The strength of pure centrifugal casted aluminium alloy sample was 143.2 (MPa). As it clearly

indicates in **Fig.4.14** the strength is still higher than the fabricated Fe-Al, and the reason could be that some or uneven distribution of the aluminium alloy in the interphase boundaries, defects there and bad bonding between lattice and aluminium influence the mechanical properties of the composite.

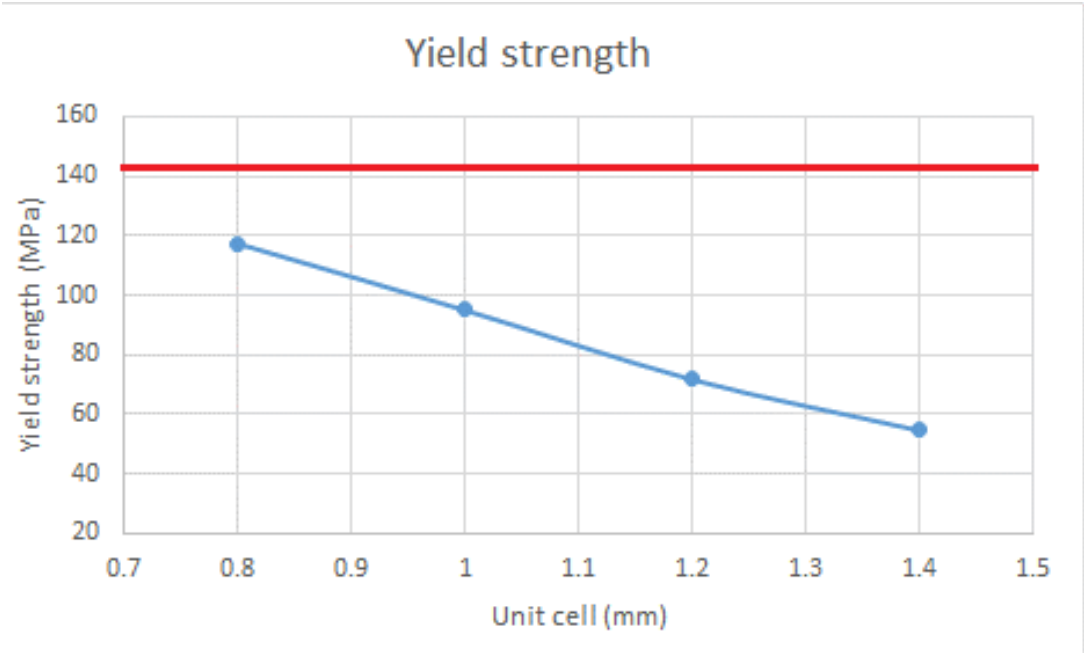

Fig. 4.14 – Yield strength.

Special attention should be put on the interphase Fe-Al boundaries Fig 4.9, because bonding strength between matrix and reinforcement is defining strength of the material.

5. Conclusions

The present study is focused on investigation of the Architected Interpenetrating Composite materials manufactured by SLM in combination with centrifugal casting and SPS. The lattice structures were designed in RDesigner software with unit cell size of 0.8 mm, 1 mm, 1.2 mm, and 1.4 mm. The effect of unit cell size on the manufacturability, density, yield strength and compression properties were investigated. The influence of powder particles size, layer thickness and other SLM process parameters were estimated, and optimal process parameters was chosen. Based on the study the next conclusions could be done:

- The layer thickness is one of the most important parameters to optimize the SLM process in case of not standard initial powders. In our case only 70mm layer was optimal and worked fine.
- Big layer thickness and spherical-like shape of melt pool in each layer caused smaller re-melted area on the previous layer and as a result weaker connection between two neighbouring layers.
- Iron lattices with unit cell size starting from 1.2 mm have a potential to be used as an energy absorbers due to specific deformation and destroying mechanism which was observed.
- After embedding of iron lattices with aluminium alloy AlSi7Mg, strength values increased 4, 8, 11 and 22 times for samples with unit cell size 0.8 mm, 1 mm 1.2 mm, 1,4 mm and 1.4 mm respectively but all these values were lower compare to reference sample made of pure aluminium alloy without lattice.
- Several defects on the interphase boundaries between iron lattice and aluminium matrix was observed. Big and small gaps in that specific place are influencing interphase bonding strength and as a result mechanical properties of the composite. Mechanical properties could be improved with improving interphase connection of iron lattice and aluminium.
- The study were performed as preliminary investigation of new type of metal-metal architectured IPC composite materials based on iron lattice structures. It was proved that it is possible to produce such metal-metal architectured IPC composites, however to improve their mechanical performance further investigations should be done.

6. Resume

The present study is focused on investigation of the Architected Interpenetrating Composite materials manufactured by SLM in combination with centrifugal casting and SPS. With optimal powder layer thickness of 70 µm the SLM process of non-standard for AM iron powder can be successfully performed. Lattices were created using Realiser RDesigner software. Generated lattice structure consists of connected vectors with zero thickness. Unit cell size of lattice structures was 0.8 mm, 1 mm, 1.2 mm, 1,4 mm and 1.6 mm were used to prepare the Architected Interpenetrating Composites.

Conventional method involved mixing the raw aluminium and iron powder and pressing with SPS. Difference in methodology of SLM process is printed iron lattices and infiltrated with aluminium. This is achieved by centrifugal casting and also SPS.

As we compare SPS and centrifugal casting approaches for producing composites, we can assume that SPS is better in mechanical properties, but during the process under pressure lattice structure is deforming. With centrifugal casting we can avoid lattice shape changes and keep the initial lattice architecture in the final composite.

SEM investigations of the obtained composites shows two phases, aluminium matrix and iron lattice. However, on the interphase boundaries of the SPS processed samples the third phase was observed. However, after etching, some gaps appeared on the interphase boundaries in the same places where third phase was located before. It is possible that the third phase is just mechanical mixture of iron and aluminium micro-particles. Also, the same gaps were observed in the centrifugally casted samples, the places of gaps locations were same - interphase boundaries between lattice and aluminium.

The study were performed as preliminary investigation of new type of metal-metal architected IPC composite materials based on iron lattice structures. However to improve the mechanical performance of the composites further investigations should be done. Further investigations should be focused on improving the interphase connection between lattice structure and matrix material.

7. Resümee

Käesolev töö uurib täiustatud ülesehitusega sissetungivaid faasilisi komposiitmaterjale, mis on valmistatud selektiivse laser sulatuse (SLM) meetodil koos tsentrifugaalvalu ja plasma-aktiveeritud paagutusga (SPS). Printimisprotsessis kasutati printimiseks mitte mõeldud raua pulbrit, millega suudeti valmistada katsekehad kihipaksusega 70 µm. Võrestruktuurid genereeriti kasutades printimisseadme tootja Realizer GmbH tarkvara RDesigner, mis koosneb null paksusega vektoritest. Baasvõre suuruseks valiti 0,8 mm – 1,6 mm mida kasutati täiustatud ülesehitusega sissetungiva faasilise komposiitmaterjalide valmistamiseks.

Tavapärane meetod antud komposiitide valmistamise puhul on lähtepulbrite (antud juhul alumiiniumi ja raua) segamine ja paagutamine SPS ahjuga. Käesolevas töös tehakse kõige pealt raua võrestik SLM printeriga ning seejärel infiltreeritakse alumiiniumiga. Infiltreerimine saavutatakse tsentifugaalvalu ning palsma-aktiveeritud paagutusega.

Võrreldes SPSi ja tsentrifugaalvalu komposiitide valmistamiseks on näha, et SPS tehnoloogia puhul on materjali mehaanilised omadused paremad, kuid samal ajal toimub antud protsessi puhul võre deformeerimine. Tsentrifugaalvalu korral ei toimu algse rauavõre kuju deformatsiooni.

Elektronmikroskoopi all täheldati komposiitmaterjalis kahte faasi – alimiiniumist maatriks ning rauast võrestik. Materjalid tehtud SPS meetodiga omasid ka kahe faasi piiril kolmandat faasi. Samas peale söövitamist faasidevaheline kolmas faas kadus ning tekkisid tühimikud võrestiku ja maatriksi vahele. On võimalik, et tekkinud kolmas faas on mehaaniline segu rauast ja alumiiniumist. Tsentrifugaalvalu korral oli kahe vaasi vahel näha tühimikke, mis võib olla tingitud kehvast maatriksi märgumisest või ebapiisavast võrestiku täitmisest alumiiniumiga.

Uurimistöö on teostatud esmase uuringuga valmistamaks uut tüüpi täiustatud ülesehitusega sissetungivaid faasilisi komposiitmaterjale, mis baseeruvad rauast võrestikul. Parandamaks materjali mehaanilisi omadusi vajab komposiitmaterjal veel edasisisi uuringuid. Edasistel uuringutel tuleks fokuseerida kahe faasi vahelise ühenduse tugevadmisele võre ja maatriksi vahel.

8. References

[1] R. K. A. A.-R. a. R. R. Oraib Al-Ketan, "Mechanical Properties of a New Type of Architected Interpenetrating Phase Composite Materials," *Advanced material technology ,* 7 December 2016.

[2] R. K. A. A.-R. a. *. A. S. D. a. H. A. Y. a. A. A. G. a. T. K. S. b. Diab W. Abueidda a, "Electrical conductivity of 3D periodic architectured interpenetrating phase composites with carbon nanostructured-epoxy reinforcements," *Composites Science and Technology,* vol. 118, pp. 127-134, 30 October 2015.

[3] b. L. H. H. S. L. B. Y. D. R. Chunze Yana, "Evaluation of light-weight AlSi10Mg periodic cellular lattice structures fabricated via direct metal laser sintering," *Journal of Materials Processing Technology,* vol. 214, no. 4, pp. 856-864, April 2014.

[4] L. H. A. H. D. R. Chunze Yana, "Evaluations of cellular lattice structures manufactured using selective laser melting," *International Journal of Machine Tools and Manufacture,* vol. 62, pp. 32-38, November 2012.

[5] b. L. H. A. H. P. Y. J. H. W. Z. Chunze Yana, "Microstructure and mechanical properties of aluminium alloy cellular lattice structures manufactured by direct metal laser sintering," *Materials Science and Engineering ,* vol. 628, pp. 238-246, March 2015.

[6] b. L. M. b. S. L. Y. T. E. M. b. J. M. b. B. M. S. G. b. F. M. R. W. d. D.A. Ramireza, "Open-cellular copper structures fabricated by additive manufacturing using electron beam melting," *Materials Science and Engineering: A,* vol. 528, no. 16-17, pp. 5379-5386, 25 June 2011.

[7] W. D. Callister, "Materials Science and Engineering: An Introduction," Vols. 7th edition, John Wiley and Sons, Inc. New York, , no. Section 4.3 and Chapter 9. , 2007.

[8] W. B. Pearson, A Handbook of Lattice Spacings and Structures of Metals and Alloys,, Newyork.

[9] A. M. Russel, "Ductility in Intermetallic Compounds," *Advanced engineering materials ,* vol. 5, no. 9, 2003.

[10] *. S. S. R. M. ,. J. S. K. E.Godlewskaa, "FeAl materials from intermetallic powders," *Intermetallics,* vol. 11, no. 4, pp. 307-312, April 2003.

[11] I. powder, "Wikipedia," [Online]. Available: https://en.wikipedia.org/wiki/Iron_powder .

[12] a. powder, "Wikipedia," [Online]. Available: https://en.wikipedia.org/wiki/Aluminium_powder .

[13] C. L. b. S. D. c. N.S. Stolo? a, "Emerging applications of intermetallics," no. Department of Materials Science and Engineering, Rensselaer Polytechnic Institute, 110 8th Street, Troy, NY 12180-3590, USA bMetals and Ceramics Division, Oak Ridge Nationa.

[14] M. M. S. Subramanian Senthilkannan Muthu, Handbook of sustainability in additive manufacturing, Volume 1 .

[15] T. S. S. T. S. Srivatsan, Additive manufacturing: innovations, advances, and applications, New york : CRC press.

[16] Y.-C. Hagedorn, Manufacturing of high performance oxide ceramics via selective laser melting = Additive Herstellung von hochfesten Oxidkeramiken mittels Selective Laser Meltings, 2013.

[17] S. paterns, "inside metal additive manufacturing," [Online]. Available: http://www.insidemetaladditivemanufacturing.com/blog/-scanning-patterns-in-slm.

[18] P. F. C. J. S. D. o. E. Eleftherios Louvis, "Selective laser melting of aluminium components," *Journal of Materials Processing Technology,* vol. 211, no. 2, pp. 275-284, 1 February 2011.

[19] M. J. Z. N. Zhijian Shen, "Spark Plasma Sintering of Alumina," Vols. 10.1111/j.1151-2916.2002.tb00381.x, August 2002.

[20] S. D. D.L. Joslin. D.S. Easton. C.T. Liu, "Reaction synthesis of FeAl alloys," *Materials Science and Engineering: A,* Vols. 192–193, Part 2,, Pages 544-548, pp. 544-548, 28 February 1995.

[21] L. C. Z. Y. W. K. a. L. X. C. o. M. S. a. E. C. U. C. XIE Yong, "Centrifugal casting processes of manufacturing in situ functionally gradient composite materials of Al-19. Si-5Mg alloy".

[22] OM, "yourarticlelibrary," [Online]. Available: http://www.yourarticlelibrary.com/micro-biology/working-principle-and-parts-of-a-compound-microscope-with-diagrams/2650.

[23] SEM, "serc.carleton.edu," [Online]. Available: http://serc.carleton.edu/research_education/geochemsheets/techniques/SEM.html.

[24] A. M. Rene Van Grieken, Handbook of X-Ray Spectrometry, Second Edition.

[25] XRD, "serc.carleton," [Online]. Available: http://serc.carleton.edu/research_education/geochemsheets/techniques/XRD.html .

[26] Vickers, "gordonengland," [Online]. Available: http://www.gordonengland.co.uk/hardness/vickers.htm.

[27] 2. M. K. M. D. S. K. I. T. F.-J. Gürtler1, "Influence of powder distribution on process stability in laser beam melting," [Online]. Available: https://sffsymposium.engr.utexas.edu/sites/default/files/2014-087-Guertler.pdf.

[28] S. CHOI, *A micromechanics method to predict the fracture toughness of cellular materials.*

[29] X.-Q. F. a. T.-H. L.-W. Yu, "Effective Elastic and Plastic Properties of Interpenetrating Multiphase Composites," *Composite Materials,* no. doi:10.1023/B:ACMA.0000003972.32599.0c, 2004.

[30] S. N. S. a. S.-H. C. Jiing-Kae Wu, “Modeling and Optimization of Two-Stage Composite Cure with the Use Open-Mold Tooling”.

[31] A. principle, “wikipedia,” [Online]. Available: https://en.wikipedia.org/wiki/Archimedes%27_principle.